

# Precision Phenomenology and New Physics Probes at Future Colliders

Dissertation Talk

Kaan Simşek

*Committee members:*

John Joseph M. Carrasco  
André Luiz de Gouvêa  
Francis John Petriello

June 16, 2025



# Prelude



# Position at the time

Particle physics at a crossroads in the  
quest to uncover physics beyond the  
Standard Model.

# Position at the time

Particle physics at a crossroads in the quest to uncover physics beyond the Standard Model.

Standard Model:

- Successfully describing known particles and their interactions
- Complete spectrum with the discovery of Higgs in 2012
- No conclusive evidence for new particles

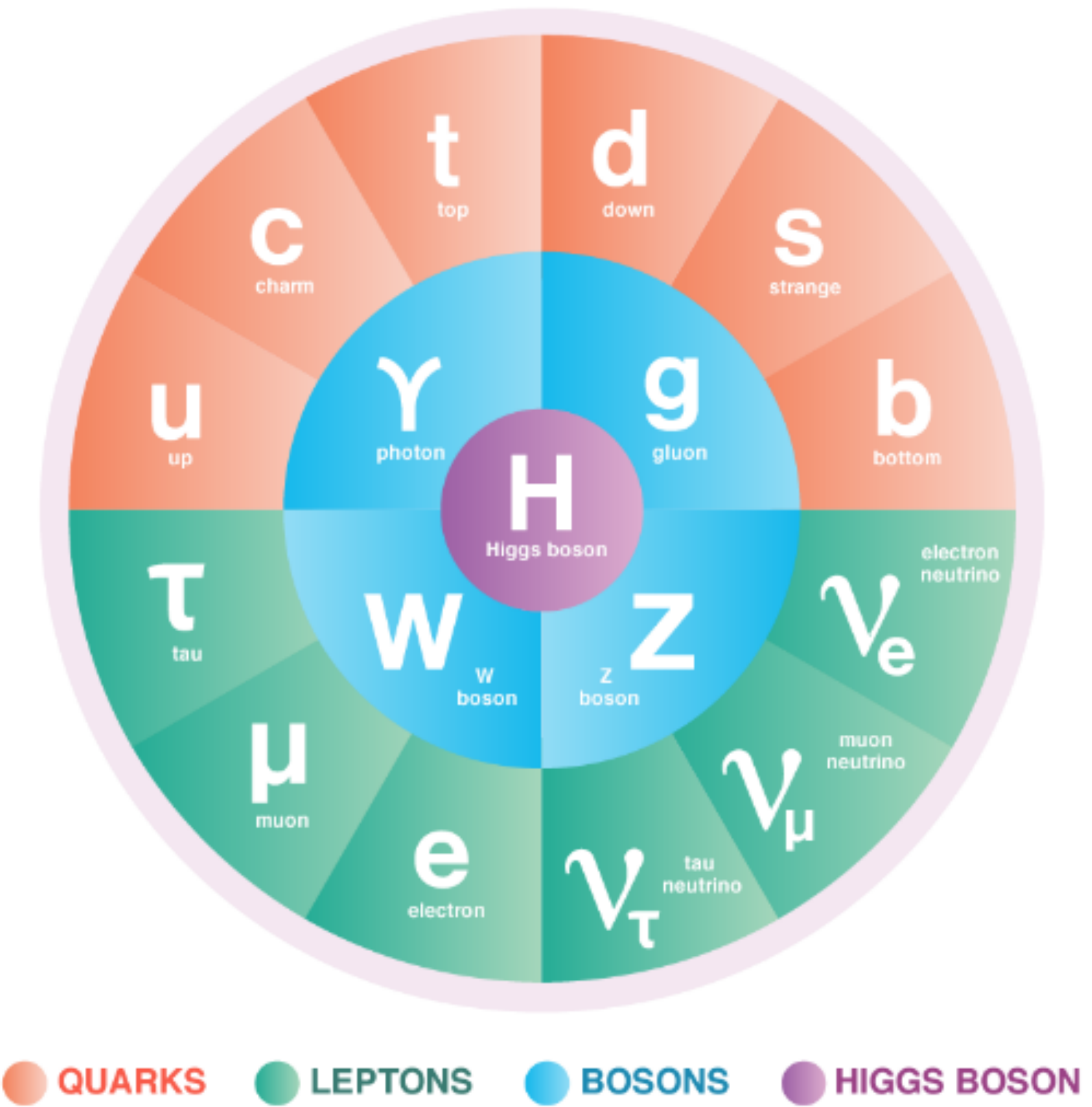
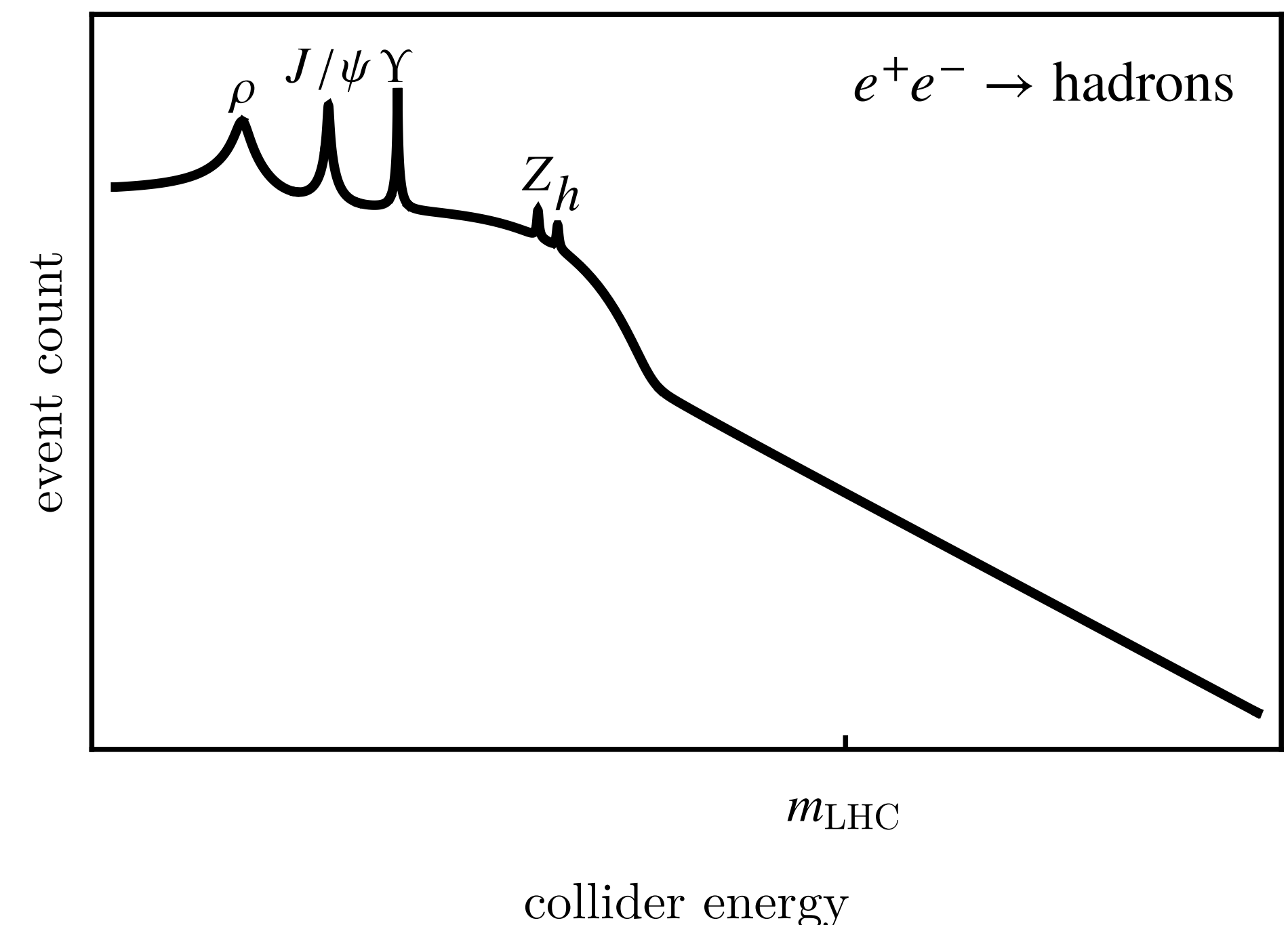


Image credit energy.gov

# Position at the time

No clear new signals



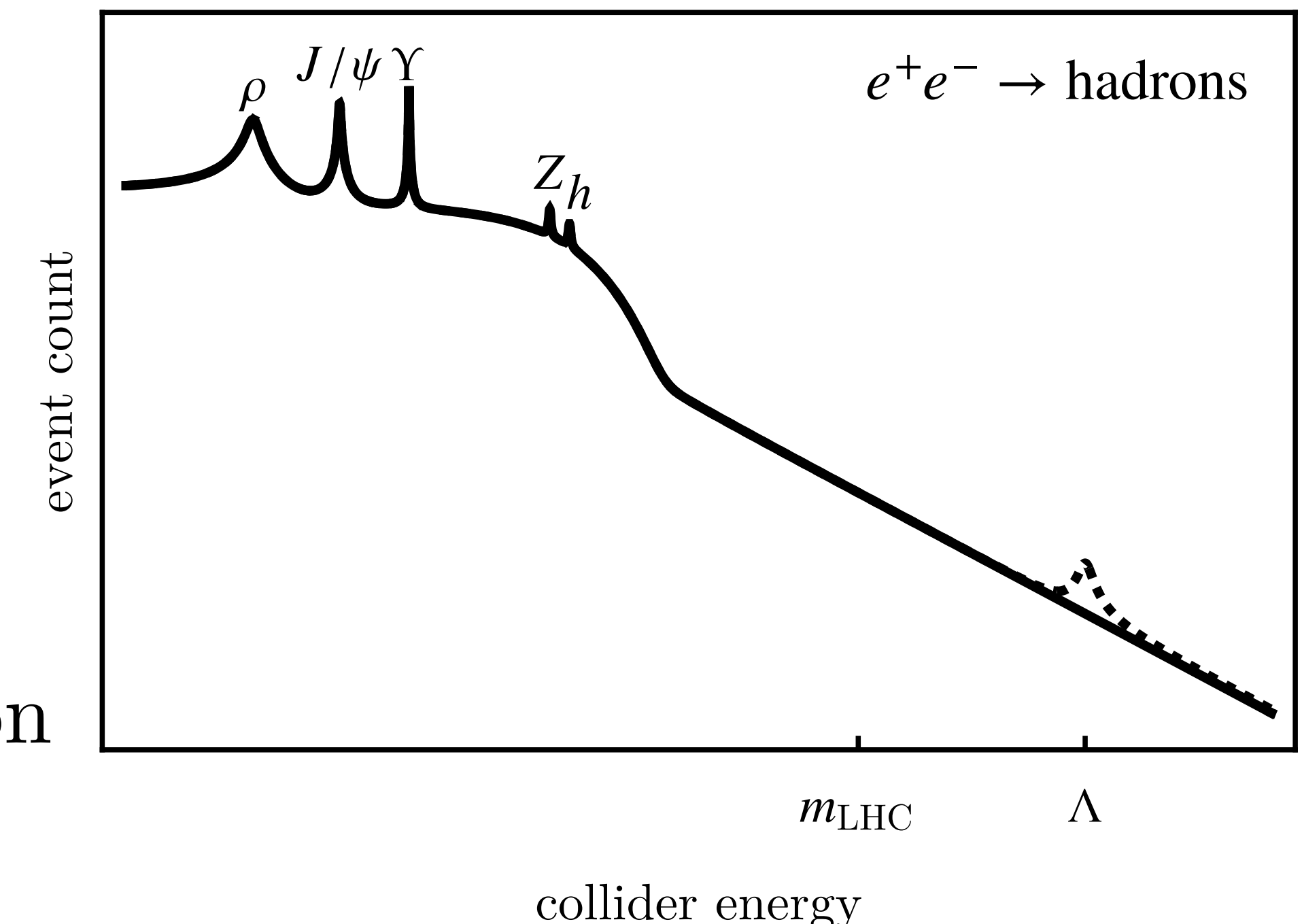
# Position at the time

No clear new signals

⇒ new physics must be heavy,  $\Lambda > m_{\text{LHC}}$ , or weakly coupled, hiding subtly within precise measurements

⇒ precision pheno is a powerful approach to indirectly probe new physics

⇒ need for bigger machines with utmost precision



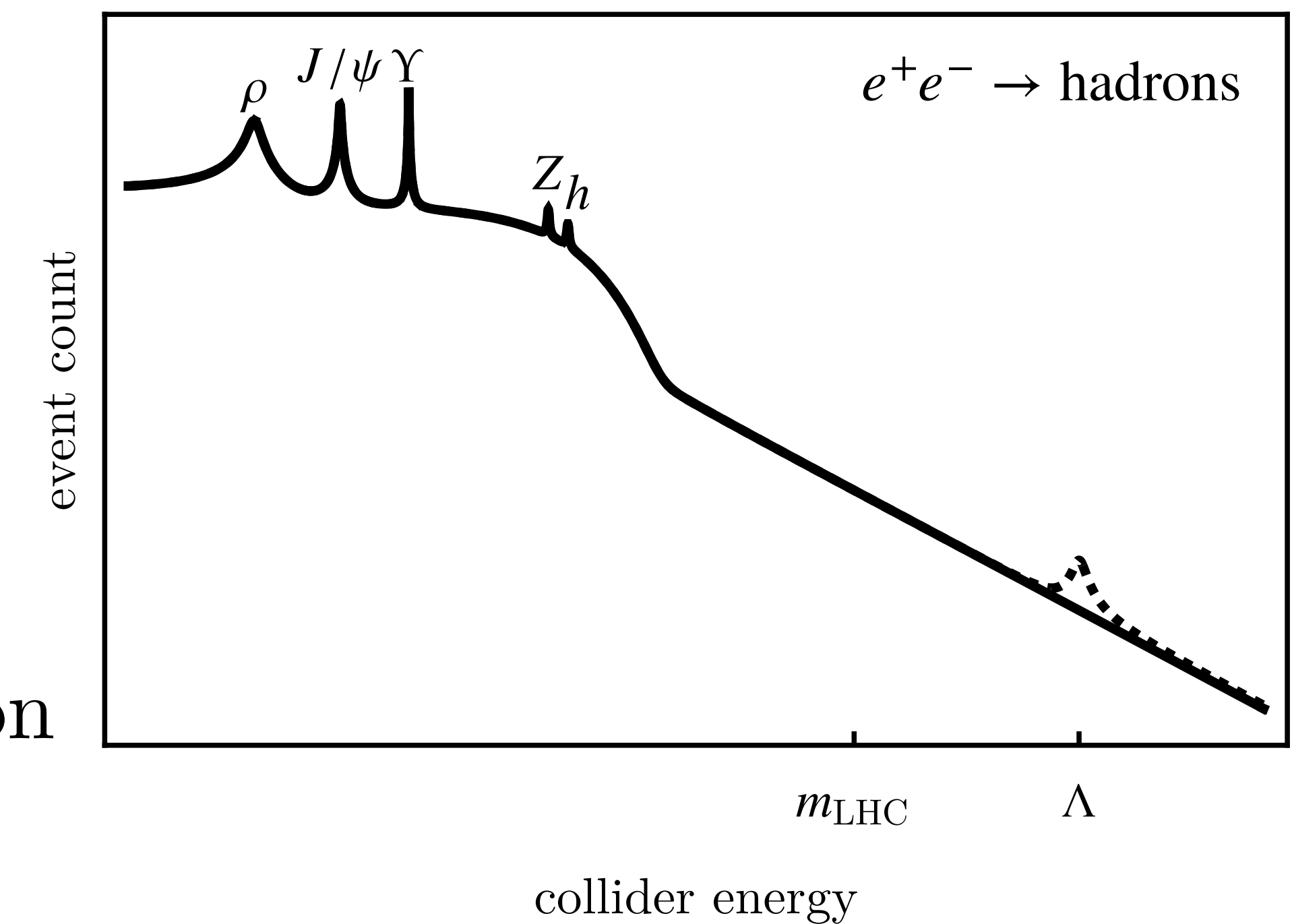
# Position at the time

No clear new signals

⇒ new physics must be heavy,  $\Lambda > m_{\text{LHC}}$ , or weakly coupled, hiding subtly within precise measurements

⇒ precision pheno is a powerful approach to indirectly probe new physics

⇒ need for bigger machines with utmost precision



Precision in what?

# Three key processes for precision physics

# Three key processes for precision physics

## Deep inelastic scattering (DIS)

Lepton-hadron collisions: clean QED probe of nucleon structure

Kinematics reconstructable from scattered lepton

Access to PDFs, spin structure, and EW couplings

Historically: HERA ( $e^-p$ , 1991-2007)

Future: EIC, LHeC, FCC-eh

# Three key processes for precision physics

## Deep inelastic scattering (DIS)

Lepton-hadron collisions: clean QED probe of nucleon structure

Kinematics reconstructable from scattered lepton

Access to PDFs, spin structure, and EW couplings

Historically: HERA ( $e^-p$ , 1991-2007)

Future: EIC, LHeC, FCC-eh

## Drell-Yan (DY)

Hadron-hadron collisions producing lepton pairs via virtual  $\gamma/Z$

Simple final state with high precision in dilepton invariant mass

Clean probe of EW interactions at very high energies

Backbone of precision measurements at LHC and HL-LHC

Sensitive to small deviations in kinematic distributions

# Three key processes for precision physics

**Deep inelastic scattering (DIS)**

Lepton-hadron collisions: clean QED probe of nucleon structure

Kinematics reconstructable from scattered lepton

Access to PDFs, spin structure, and EW couplings

Historically: HERA ( $e^-p$ , 1991-2007)

Future: EIC, LHeC, FCC-eh

**Drell-Yan (DY)**

Hadron-hadron collisions producing lepton pairs via virtual  $\gamma/Z$

Simple final state with high precision in dilepton invariant mass

Clean probe of EW interactions at very high energies

Backbone of precision measurements at LHC and HL-LHC

Sensitive to small deviations in kinematic distributions

We consider DY+jet (DY $j$ )!

$$pp \rightarrow j\gamma/Z^* \rightarrow je^-e^+$$

# Three key processes for precision physics

## Deep inelastic scattering (DIS)

Lepton-hadron collisions: clean QED probe of nucleon structure

Kinematics reconstructable from scattered lepton

Access to PDFs, spin structure, and EW couplings

Historically: HERA ( $e^-p$ , 1991-2007)

Future: EIC, LHeC, FCC-eh

## Drell-Yan (DY)

Hadron-hadron collisions producing lepton pairs via virtual  $\gamma/Z$

Simple final state with high precision in dilepton invariant mass

Clean probe of EW interactions at very high energies

Backbone of precision measurements at LHC and HL-LHC

Sensitive to small deviations in kinematic distributions

## $e^+e^-$ annihilation

Point-like initial state with tunable energy and beam polarization

No hadronic initial-state uncertainties

Precision measurements of  $Z$ ,  $W$ , Higgs, and top properties

Legacy: LEP, SLD

Future: FCC-ee

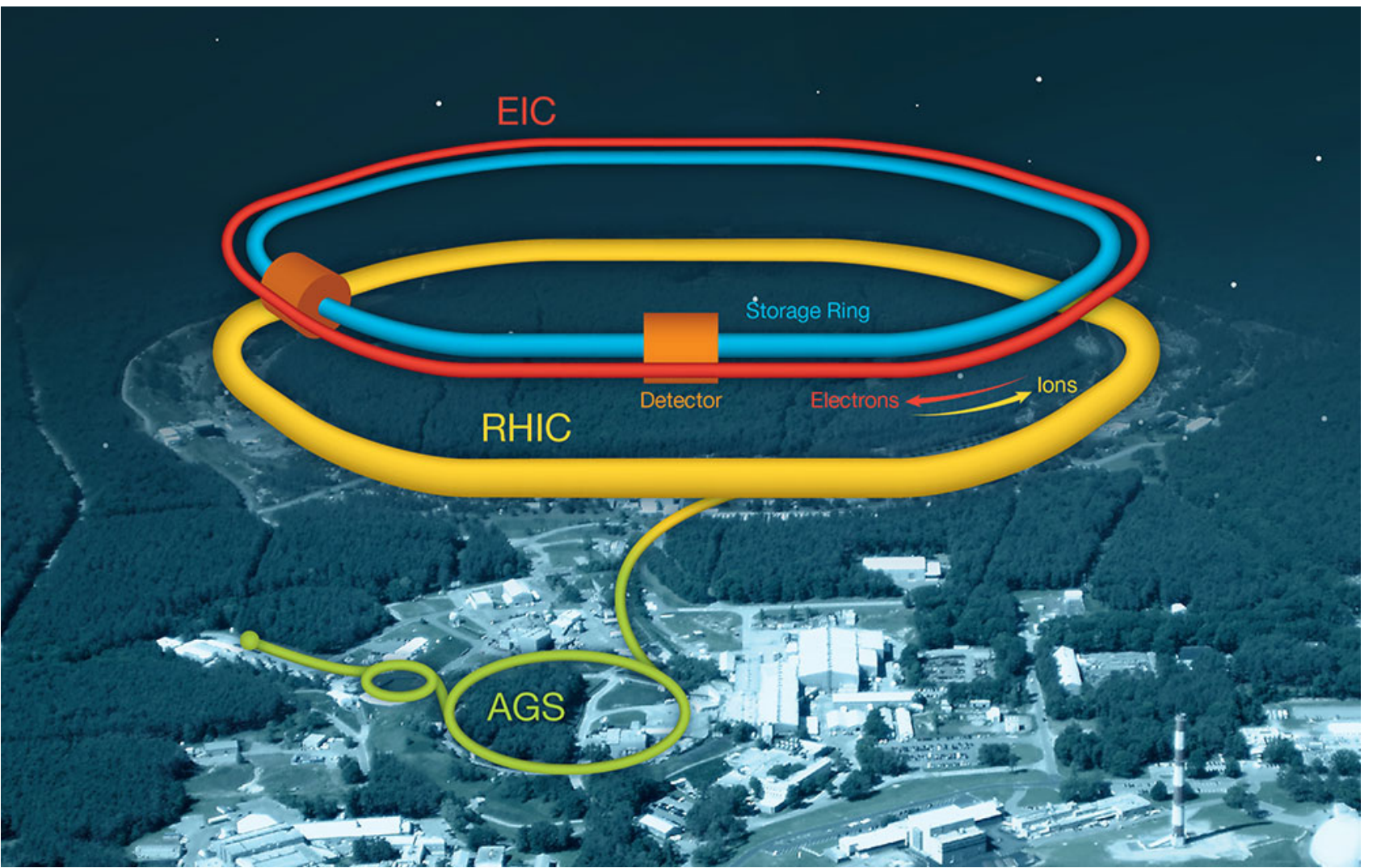
Ideal environment for ultra-clean EW physics

# Electron-Ion Collider

- At Brookhaven National Lab (BNL), NY
- First ever dedicated  $e^-A$  collider in the USA
- Collides polarized  $e^-$  with protons and light/heavy ions:  $^1H$ ,  $^2H$ ,  $^3He$ ,  $^4He$ ,  $^{197}Au$ ,  $^{238}U$
- Both beams polarized:
  - Electrons: 85% at the source, 70% in the ring
  - Ions: up to 70% for light nuclei
- Approved by DOE in 2020
- Construction starting at the end of 2025
- First collisions expected in early 2030s

# Electron-Ion Collider

- Electron beam: up to 18 GeV
- Proton beam: up to 275 GeV, heavier ions  $\leq 137$  GeV
- $\sqrt{s} = 20$  to 140 GeV
- Luminosity:  $100 \text{ fb}^{-1}/\text{yr}$  ( $\sim 1000\times$  HERA)
- Reuses RHIC tunnel (3.9 km); new electron ring added
- Physics goals:
  - 3D imaging of nucleon structure
  - Gluon saturation, small- $x$  dynamics
  - Precision electroweak observables in polarized DIS
  - Strong constraints on PDFs  $\Rightarrow$  improves precision at all colliders



# Large Hadron-electron Collider

- Proposed upgrade to LHC
- Adds a 60-GeV  $e^-$  beam in a new energy recovery linac
- Uses existing LHC 7-TeV proton beam
- First discussed in 1984 (LEP-LHC); LHeC study launched in 2007
- Conceptual design completed in 2011
- Awaiting approval; timeline tied to LHC Long Shutdown 3
- If approved, installation during 2026-2027
- Potential operation along side HL-LHC (Run 4) around 2027-2030

# Large Hadron-electron Collider

- Electron beam: 60 GeV
- Proton beam: 7 TeV
- $\sqrt{s} = 1.3$  TeV
- Luminosity:  $10 \text{ fb}^{-1}/\text{yr}$
- Polarization: Electron beam only, 80%
- Physics goals:
  - Extend PDFs to high  $x$  and high  $Q$
  - Precision Higgs,  $W$ , and top studies in clean environment
  - Explore electroweak structure at high energies via DIS
  - Strong complement to LHC measurements, especially for BSM effects in leptonic channels

# Future Circular Collider

- CERN-led long-term project for post-LHC colliders
- 91 km tunnel near Geneva; staged operation plan
- Feasibility report published May 2025
- Approval decision expected around 2027-2028
- FCC-ee: starts around 2045, runs for 15 years
- FCC-hh: follows in 2070s, 100 TeV  $pp$  collider
- FCC-eh: operates concurrently with FCC-ee
- Shared infrastructure between  $e^+e^-$ ,  $pp$ , and  $e^-p$  modes

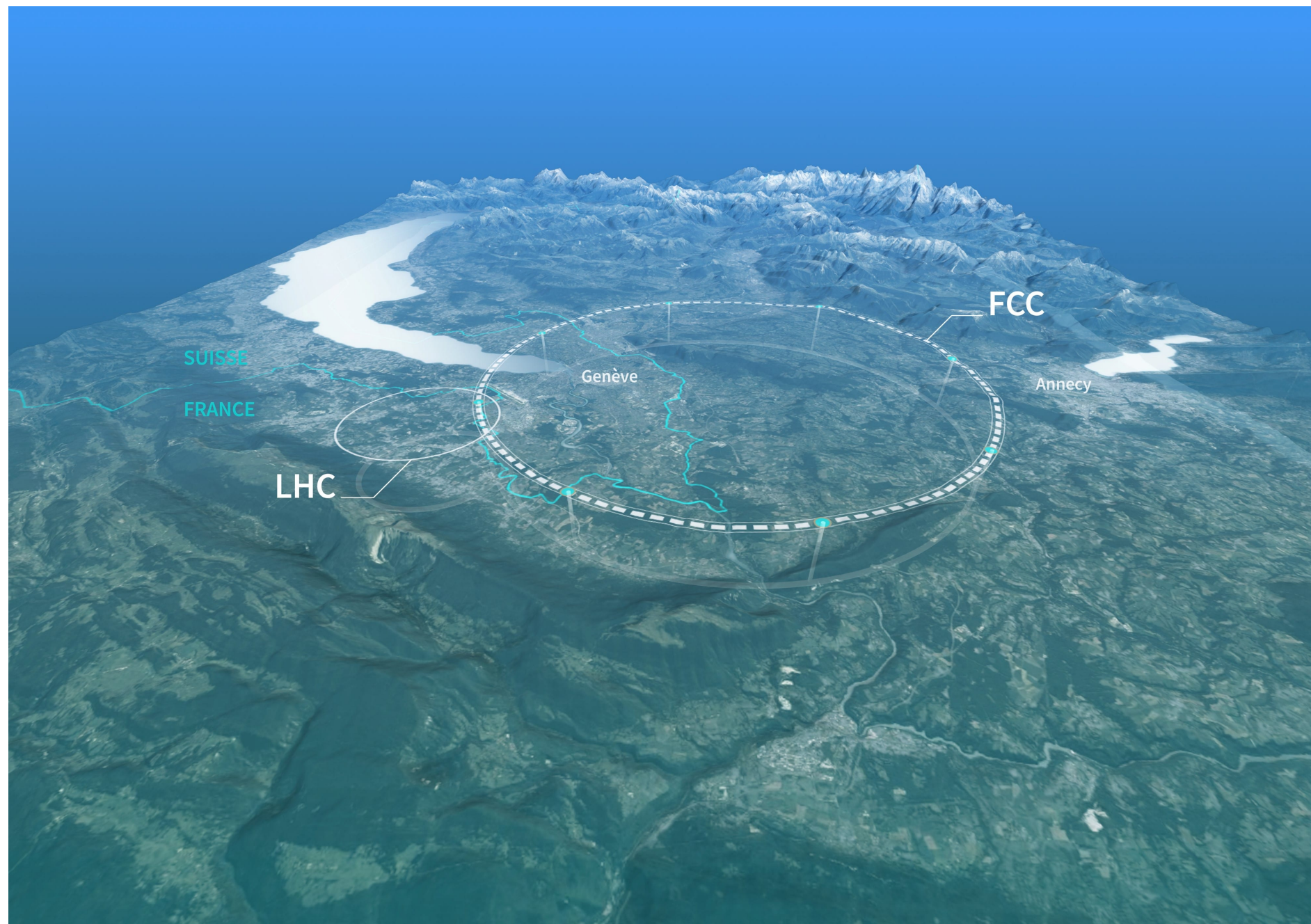


Image credit cern.ch

# Future Circular Collider

FCC-ee (lepton mode):

- $e^+e^-$  collisions at Z pole (91 GeV),  $WW$  threshold (160 GeV), Higgsstrahlung peak (240 GeV),  $t\bar{t}$  threshold (365 GeV)
- Luminosity:  $10 \text{ ab}^{-1}/\text{stage}$
- Transverse beam polarization at low energies; longitudinal optional ( $\geq 40\%$ )
- Goals: ultra-precise  $Z$ ,  $W$ , Higgs, and top studies

FCC-eh (lepton-proton mode):

- $60 \text{ GeV} \times 50 \text{ TeV } e^-p$  collisions,  $\sqrt{s} = 3.5 \text{ TeV}$
- Luminosity:  $100 \text{ fb}^{-1}/\text{yr}$
- Electron beam polarized (80%); proton beam unpolarized
- Goals: PDFs at extreme  $x$  and  $Q$ , electroweak couplings

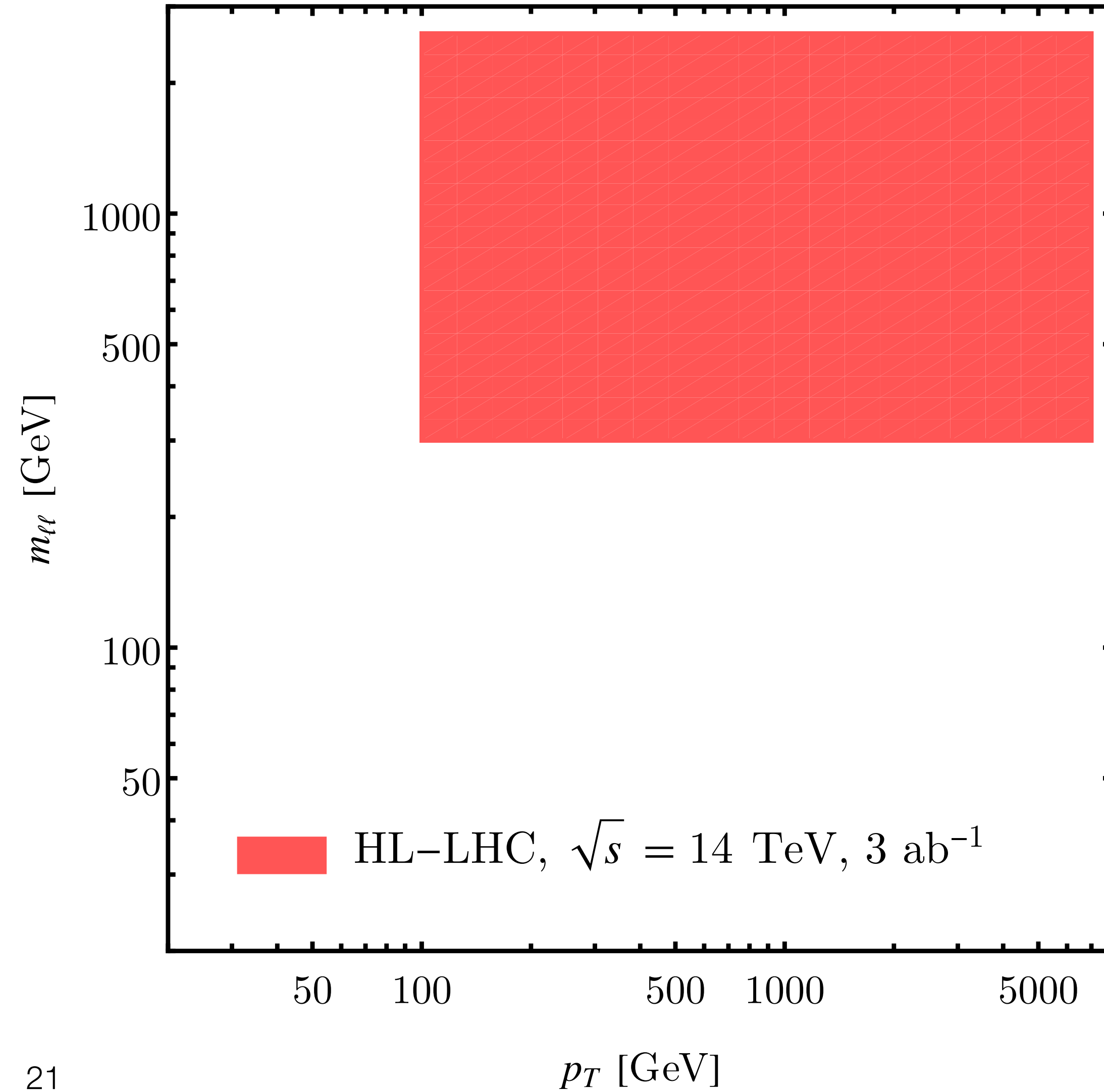
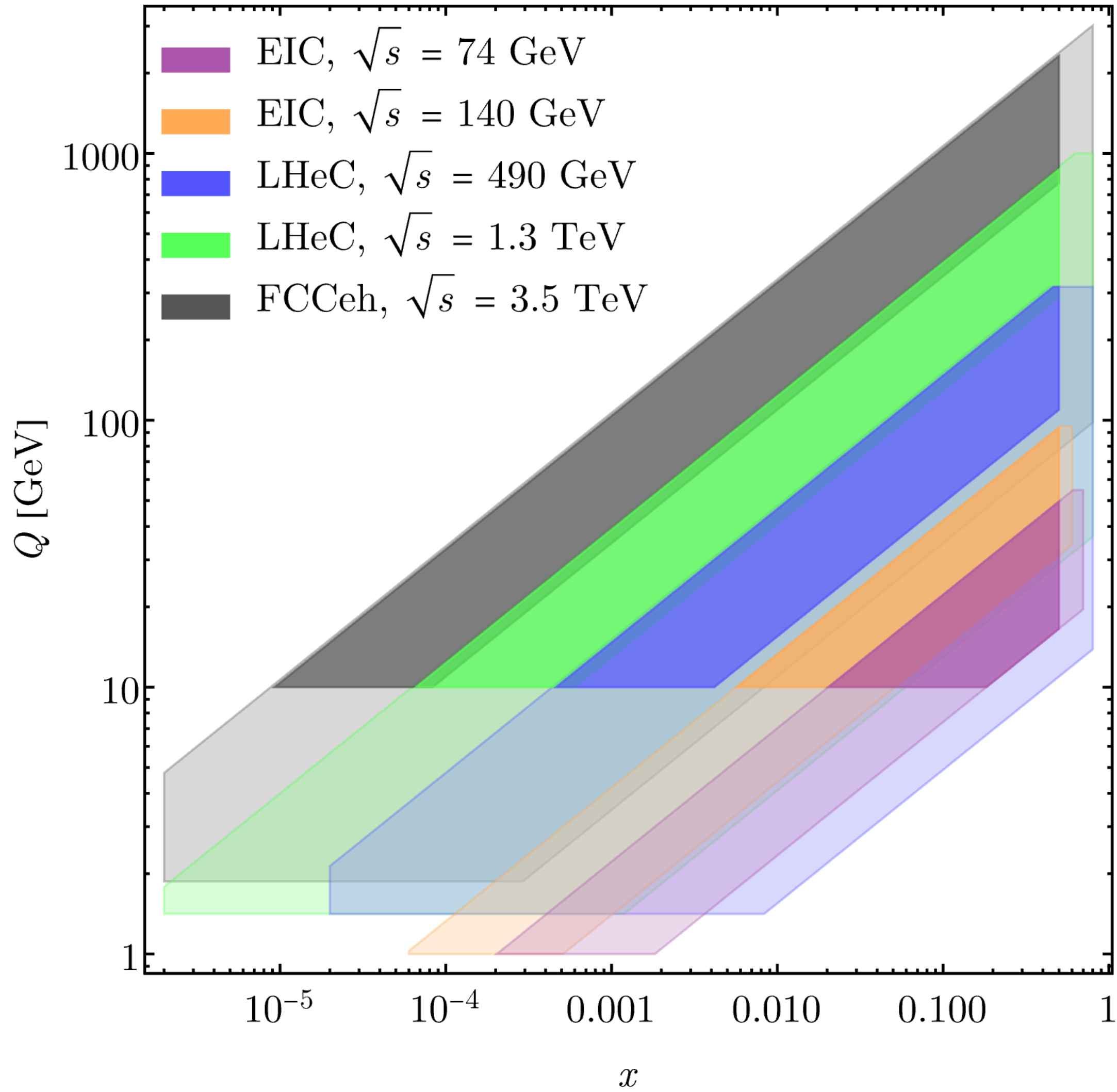
# High-Luminosity LHC

- Next-phase  $pp$  program at CERN
- Builds on current LHC, extending to around 2039
- Designed for 10× integrated luminosity:  $3 \text{ ab}^{-1}$  at 14 TeV
- Detector upgrades, improved pileup mitigation
- Focus on rare SM processes, precision, and discovery
- Major input for global fits and new physics searches

# High-Luminosity LHC

- $\sqrt{s} = 14 \text{ TeV}$
- Luminosity:  $3 \text{ ab}^{-1}$  (total)
- Unpolarized  $pp$  beams
- Physics goals:
  - Precision measurements in high-mass Drell-Yan ( $m_{\ell\ell} \gg m_Z$ )
  - Constraints on vector boson scattering, contact interactions
  - High-statistics studies of Higgs, top, Z/W
  - Direct searches and indirect probes via tail distributions

# Kinematic coverage



# Toolbox

# Standard Model Effective Field Theory

Model-independent extension of the SM Lagrangian with higher-dimensional operators  $O_k^{(n)}$  built up of SM fields at an energy scale  $\Lambda$  heavier than all SM fields and beyond accessible collider energy, introducing Wilson coefficients  $C_k^{(n)}$  as effective couplings:

$$\mathcal{L} = \mathcal{L}_{\text{SM}} + \sum_{n>4} \frac{1}{\Lambda^{n-4}} \sum_k C_k^{(n)} O_k^{(n)}$$

# Standard Model Effective Field Theory

Model-independent extension of the SM Lagrangian with higher-dimensional operators  $O_k^{(n)}$  built up of SM fields at an energy scale  $\Lambda$  heavier than all SM fields and beyond accessible collider energy, introducing Wilson coefficients  $C_k^{(n)}$  as effective couplings:

$$\mathcal{L} = \mathcal{L}_{\text{SM}} + \sum_{n>4} \frac{1}{\Lambda^{n-4}} \sum_k C_k^{(n)} O_k^{(n)}$$

Focus on  $n = 6$  for DIS  $\rightarrow$  Operators with two leptons, two quarks  
 $\rightarrow$  First leading contribution at dimension 6

# Standard Model Effective Field Theory

Model-independent extension of the SM Lagrangian with higher-dimensional operators  $O_k^{(n)}$  built up of SM fields at an energy scale  $\Lambda$  heavier than all SM fields and beyond accessible collider energy, introducing Wilson coefficients  $C_k^{(n)}$  as effective couplings:

$$\mathcal{L} = \mathcal{L}_{\text{SM}} + \sum_{n>4} \frac{1}{\Lambda^{n-4}} \sum_k C_k^{(n)} O_k^{(n)}$$

- Focus on  $n = 6$  for DIS and  $n = 8$  for DY $j$   $\rightarrow$  Operators with two leptons, two quarks, one gluon
- $\rightarrow$  We want  $p_T(\ell\ell) = p_T(V) = p_T(g)$  bins
- $\rightarrow$  gluon field strength  $\therefore$  dimension 8

# Standard Model Effective Field Theory

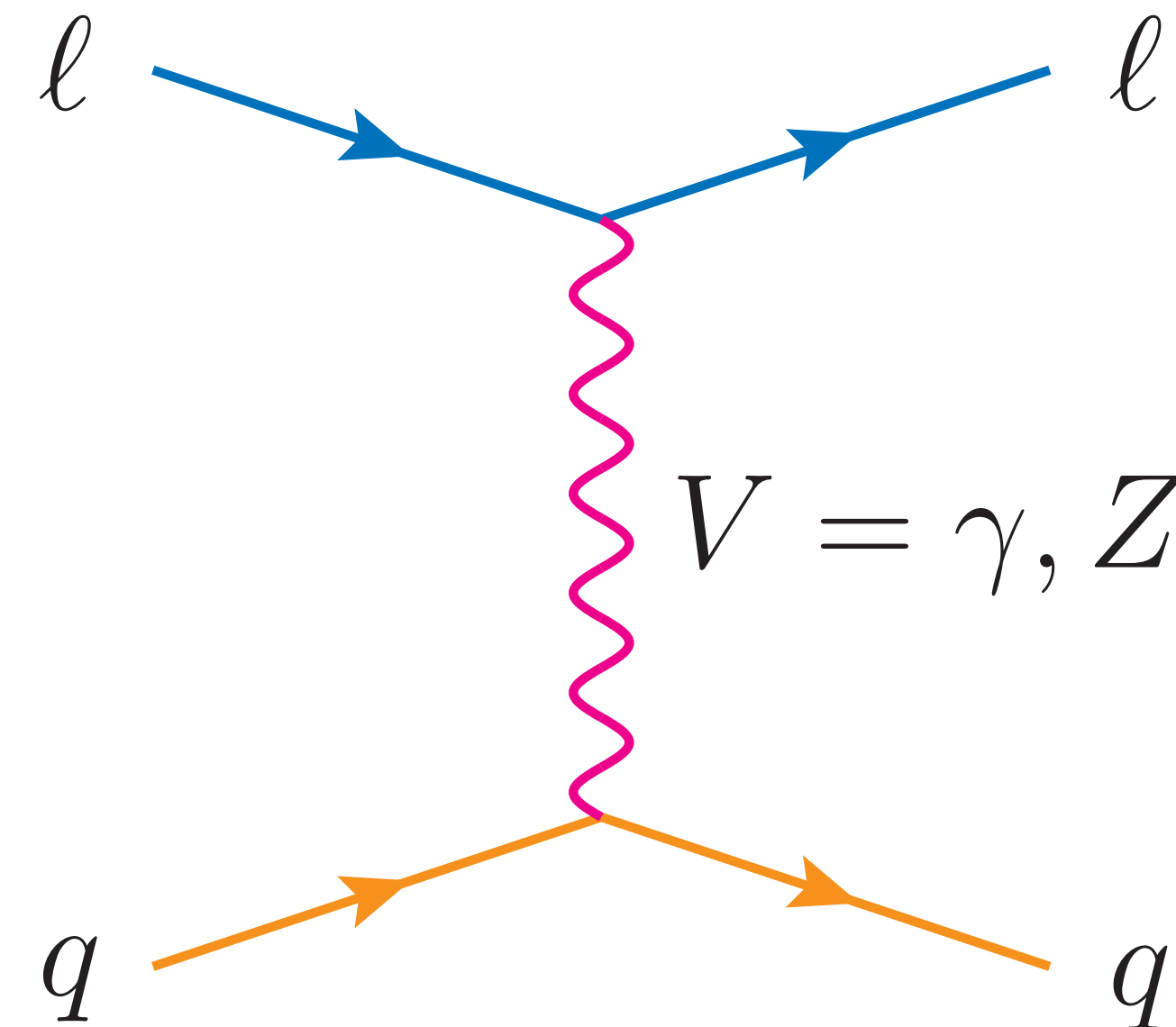
Model-independent extension of the SM Lagrangian with higher-dimensional operators  $O_k^{(n)}$  built up of SM fields at an energy scale  $\Lambda$  heavier than all SM fields and beyond accessible collider energy, introducing Wilson coefficients  $C_k^{(n)}$  as effective couplings:

$$\mathcal{L} = \mathcal{L}_{\text{SM}} + \sum_{n>4} \frac{1}{\Lambda^{n-4}} \sum_k C_k^{(n)} O_k^{(n)}$$

Focus on  $n = 6$  for DIS and  $n = 8$  for DY $j$ . Restrict to leading order SMEFT.

# Standard Model Effective Field Theory

SMEFT contributions to DIS:



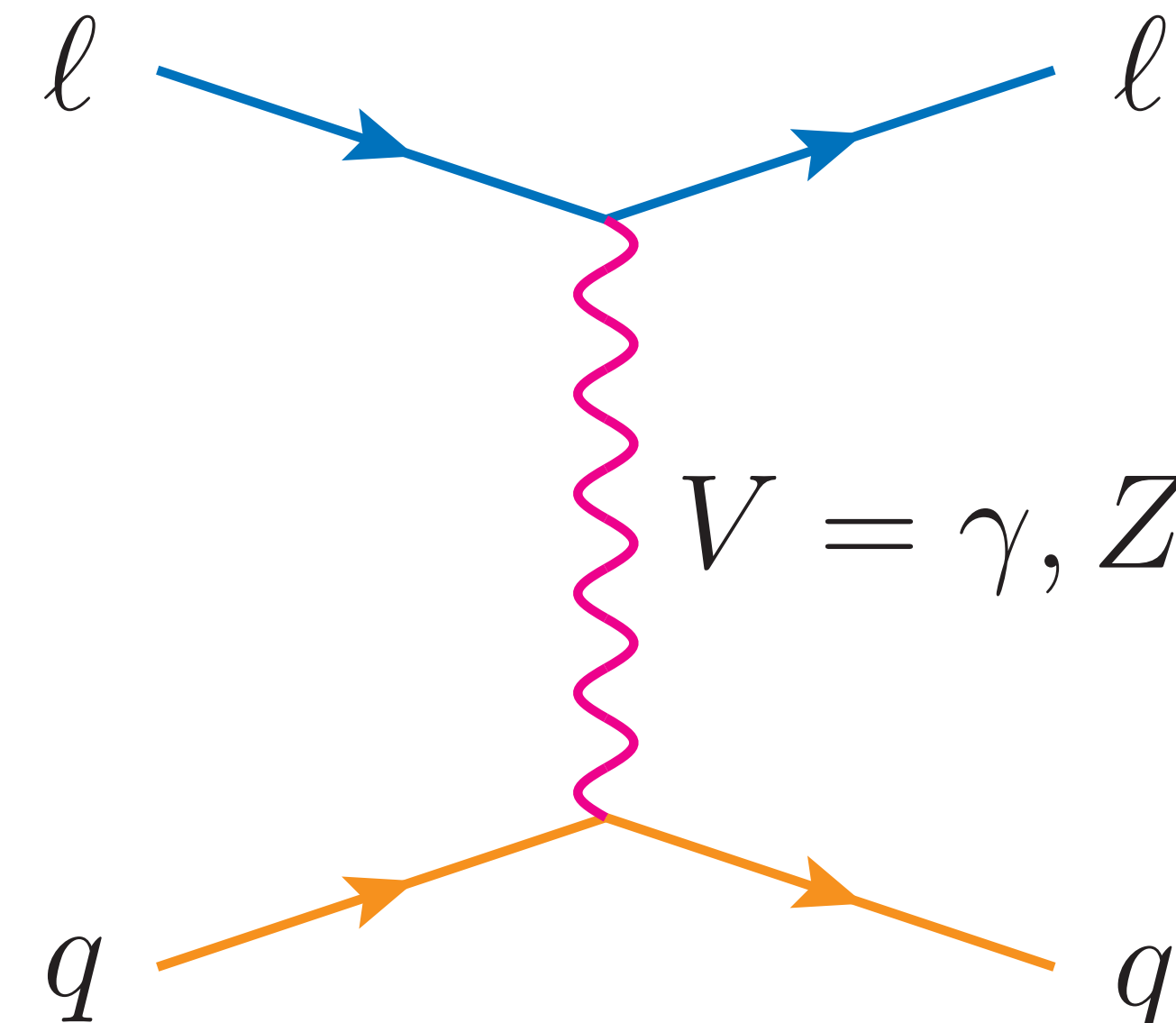
Semi-leptonic four-fermion operators:

$$O_{XY} = [\bar{\ell}\gamma^\mu P_X \ell][\bar{q}\gamma_\mu P_Y q]$$

For nontrivial SM-SMEFT interference,  
we need helicity-preserving currents.

# Standard Model Effective Field Theory

SMEFT contributions to DIS:



Semi-leptonic four-fermion operators:

$$O_{XY} = [\bar{\ell}\gamma^\mu P_X \ell][\bar{q}\gamma_\mu P_Y q]$$

For nontrivial SM-SMEFT interference,  
we need helicity-preserving currents.

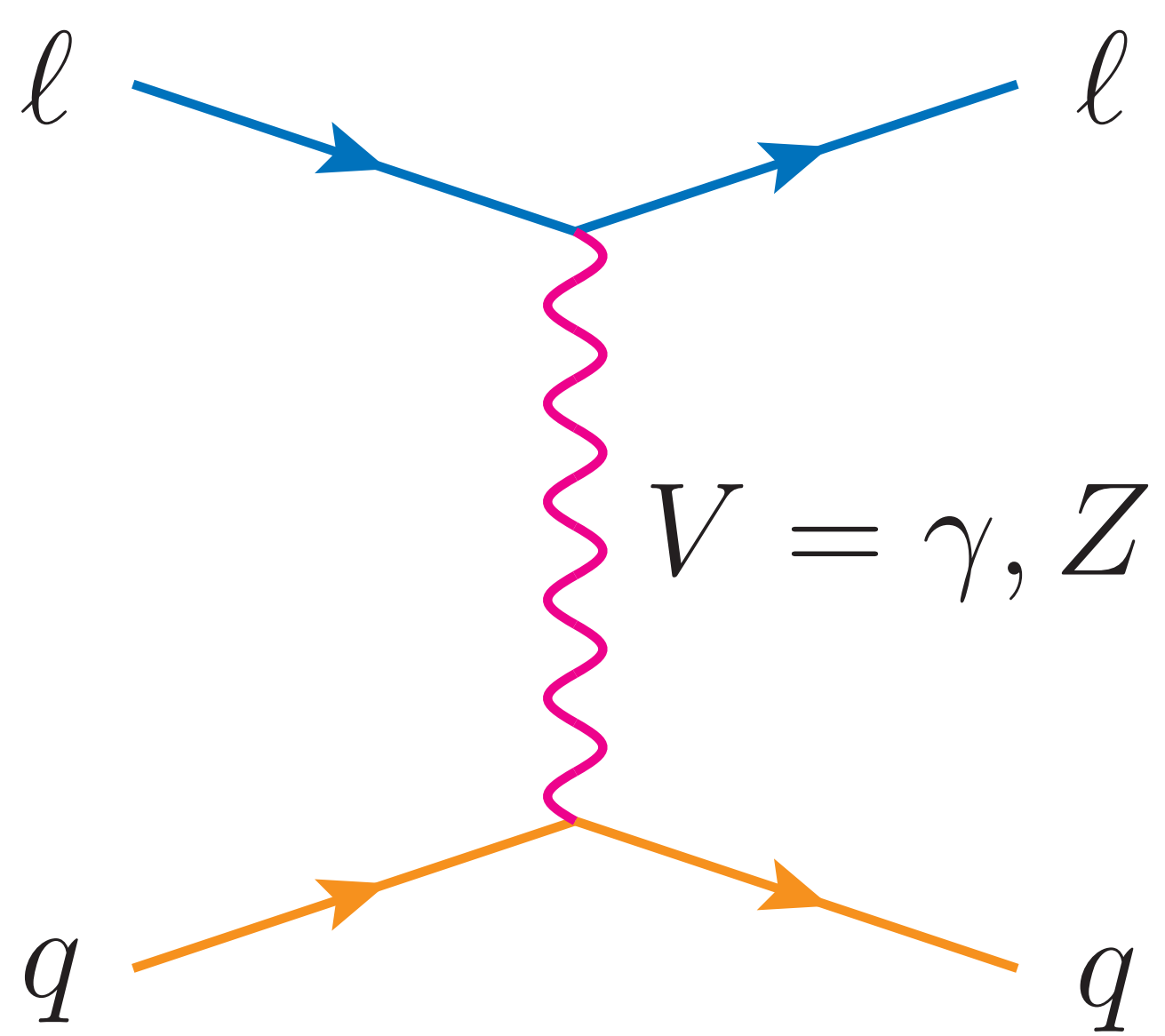
Corrections to  $ffV$  vertices:

$$V^\mu = V_{\text{SM}}^\mu \left( 1 + \sum_k C_k V_k \right)$$

SM vertices are shifted in a gauge-invariant manner.

# Standard Model Effective Field Theory

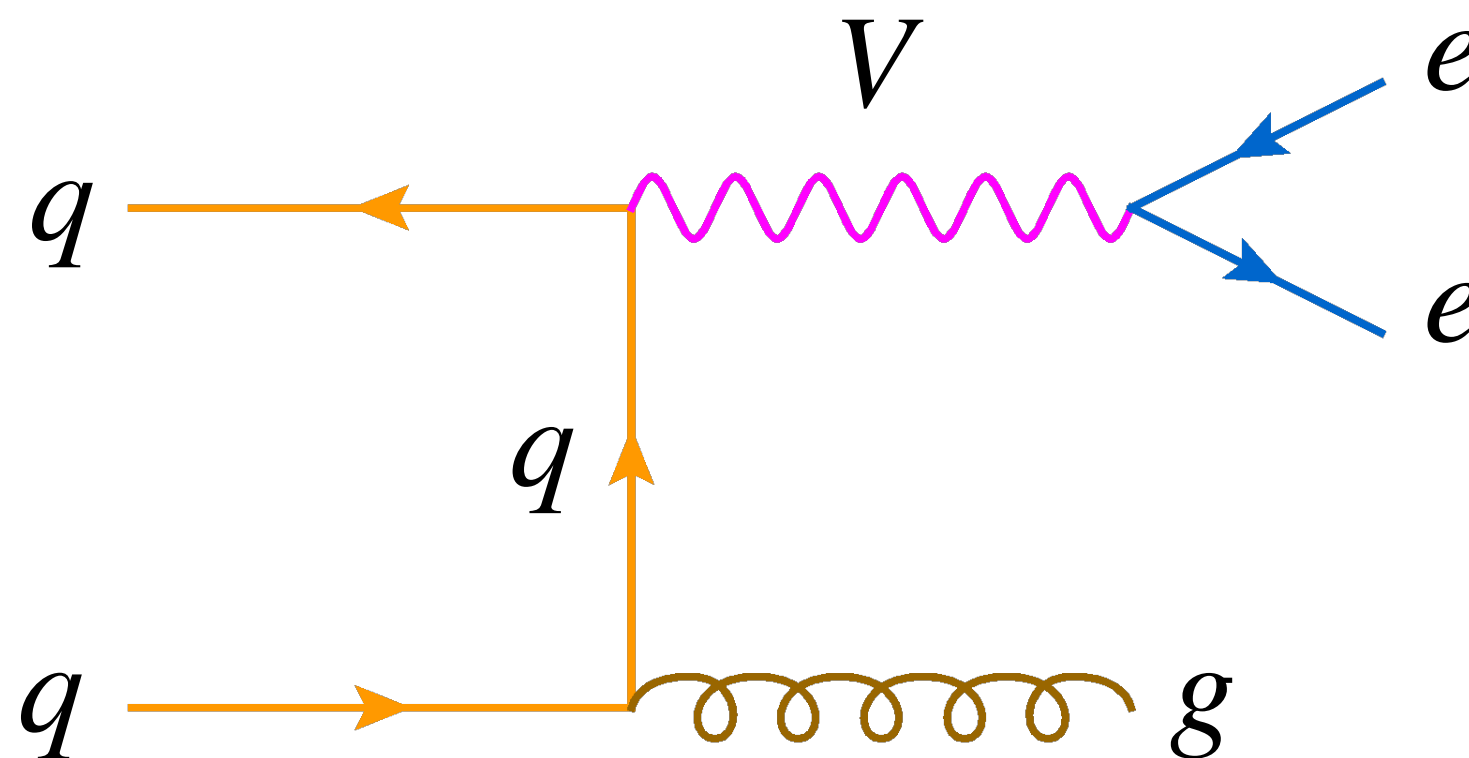
SMEFT contributions to DIS:



$ffV$	semi-leptonic four-fermion
$O_{\varphi WB} = (\varphi^\dagger \tau^I \varphi) W_{\mu\nu}^I B^{\mu\nu}$	$O_{\ell q}^{(1)} = (\bar{\ell} \gamma^\mu \ell)(\bar{q} \gamma_\mu q)$
$O_{\varphi D} = (\varphi^\dagger D^\mu \varphi)^* (\varphi^\dagger D_\mu \varphi)$	$O_{\ell q}^{(1)} = (\bar{\ell} \gamma^\mu \tau^I \ell)(\bar{q} \gamma_\mu \tau^i q)$
$O_{\varphi \ell}^{(1)} = (\varphi^\dagger i \overset{\leftrightarrow}{D}^\mu \varphi)(\bar{\ell} \gamma_\mu \ell)$	$O_{eu} = (\bar{e} \gamma^\mu e)(\bar{u} \gamma_\mu u)$
$O_{\varphi \ell}^{(3)} = (\varphi^\dagger i \overset{\leftrightarrow}{D}^\mu \tau^I \varphi)(\bar{\ell} \gamma_\mu \tau^I \ell)$	$O_{ed} = (\bar{e} \gamma^\mu e)(\bar{d} \gamma_\mu d)$
$O_{\varphi e} = (\varphi^\dagger i \overset{\leftrightarrow}{D}^\mu \varphi)(\bar{e} \gamma_\mu e)$	$O_{\ell u} = (\bar{\ell} \gamma^\mu \ell)(\bar{u} \gamma_\mu u)$
$O_{\varphi q}^{(1)} = (\varphi^\dagger i \overset{\leftrightarrow}{D}^\mu \varphi)(\bar{q} \gamma_\mu q)$	$O_{\ell d} = (\bar{\ell} \gamma^\mu \ell)(\bar{d} \gamma_\mu d)$
$O_{\varphi q}^{(3)} = (\varphi^\dagger i \overset{\leftrightarrow}{D}^\mu \tau^I \varphi)(\bar{q} \gamma_\mu \tau^I q)$	$O_{qe} = (\bar{e} \gamma^\mu e)(\bar{q} \gamma_\mu q)$
$O_{\varphi u} = (\varphi^\dagger i \overset{\leftrightarrow}{D}^\mu \varphi)(\bar{u} \gamma_\mu u)$	
$O_{\varphi d} = (\varphi^\dagger i \overset{\leftrightarrow}{D}^\mu \varphi)(\bar{d} \gamma_\mu d)$	
$O_{\ell \ell} = (\bar{\ell} \gamma^\mu \ell)(\bar{\ell} \gamma_\mu \ell)$	

# Standard Model Effective Field Theory

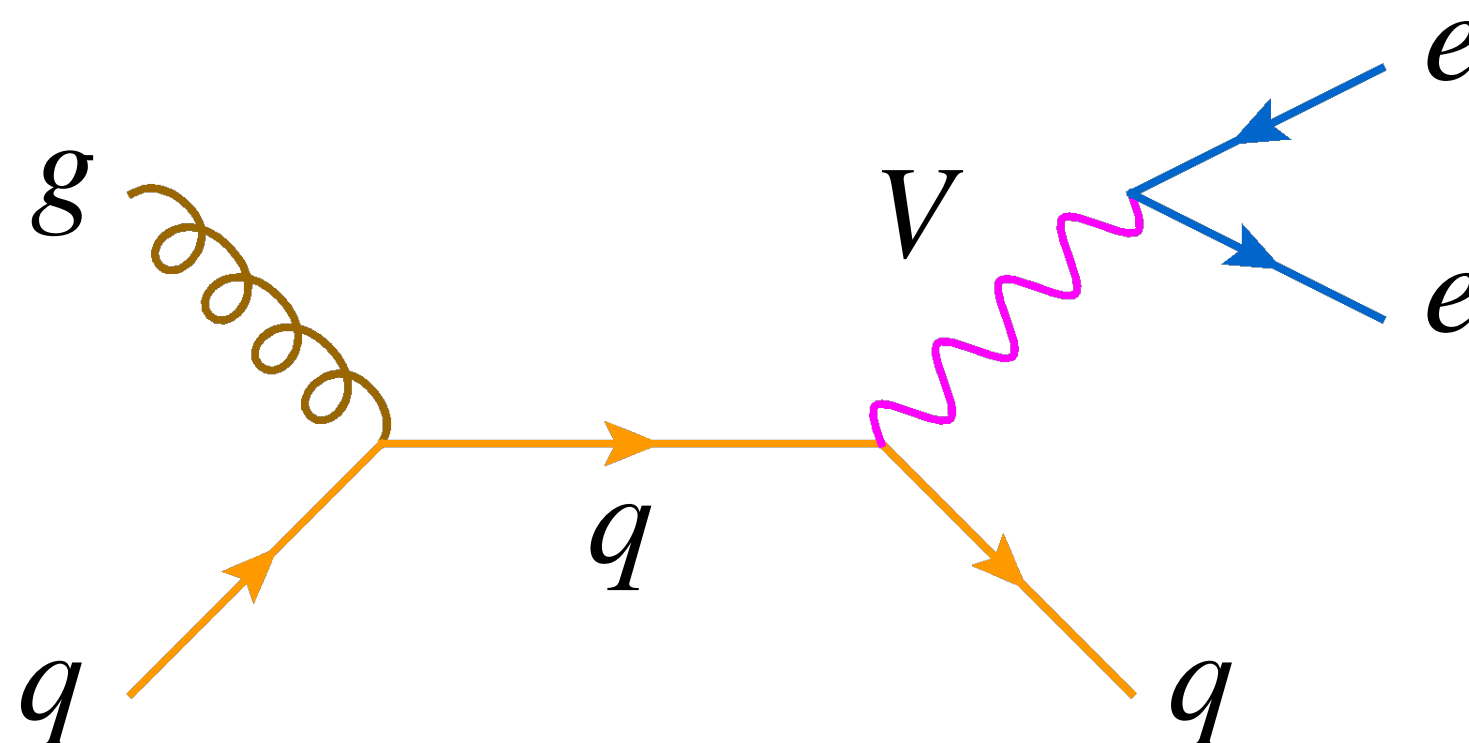
SMEFT contributions to DY $j$ :



Semi-leptonic four-fermion operators  
coupled to gluon field strength tensor:

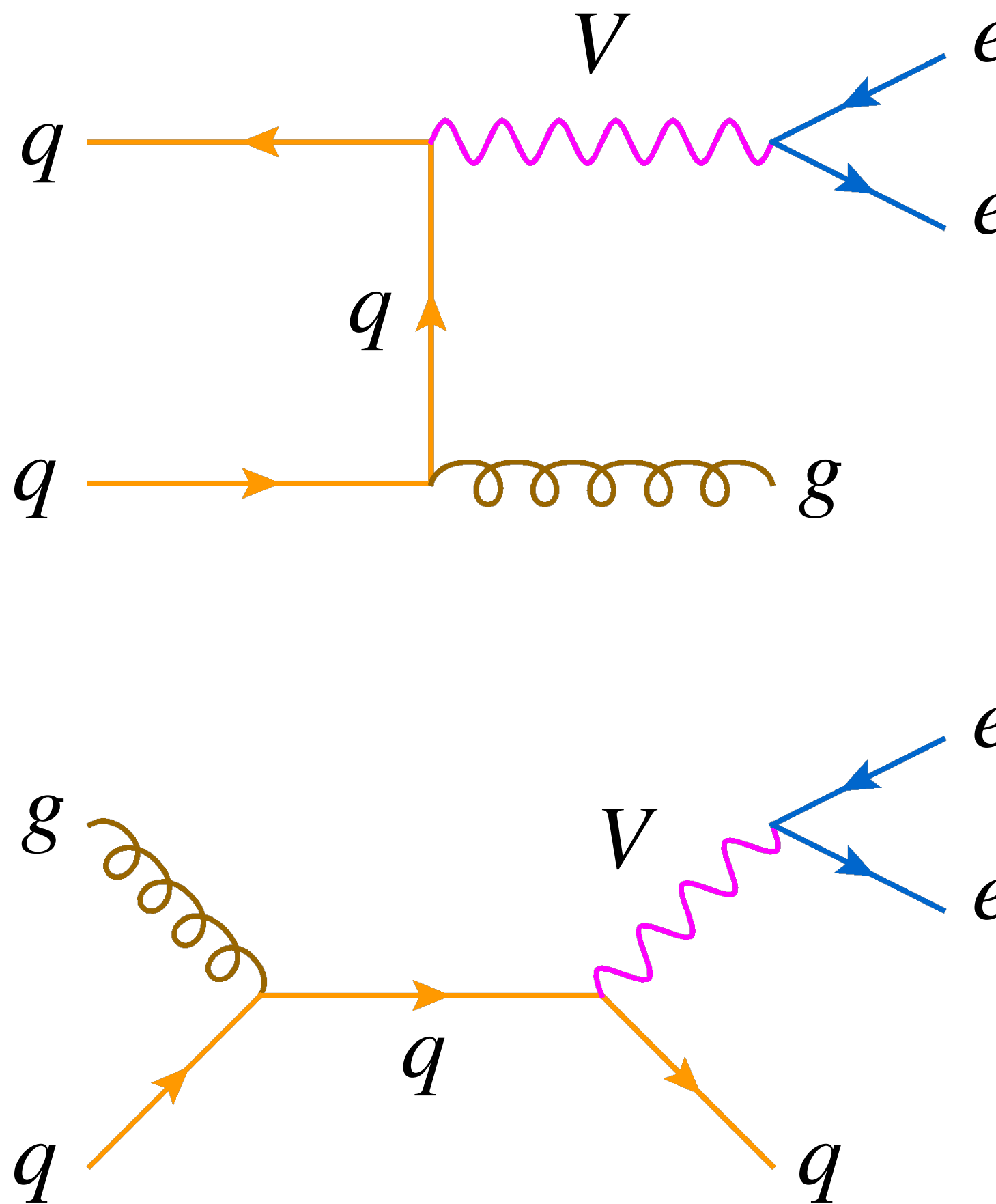
$$O_{XYg} = [\bar{\ell}\gamma^\mu P_X \ell][\bar{q}\gamma^\nu P_Y T^A q]G_{\mu\nu}^A$$

$$\tilde{O}_{XYg} = [\bar{\ell}\gamma^\mu P_X \ell][\bar{q}\gamma^\nu P_Y T^A q]\tilde{G}_{\mu\nu}^A$$



# Standard Model Effective Field Theory

SMEFT contributions to DY $j$ :



$CP$ -even		$CP$ -odd	
$\tilde{O}_{\ell^2 q^2 g}^{(1)}$	$(\bar{\ell} \gamma^\mu \ell)(\bar{q} \gamma^\nu T^a q) \tilde{G}_{\mu\nu}^a$	$O_{\ell^2 q^2 g}^{(1)}$	$(\bar{\ell} \gamma^\mu \ell)(\bar{q} \gamma^\nu T^a q) G_{\mu\nu}^a$
$\tilde{O}_{\ell^2 q^2 g}^{(3)}$	$(\bar{\ell} \tau^i \gamma^\mu \ell)(\bar{q} \tau^i \gamma^\nu T^a q) \tilde{G}_{\mu\nu}^a$	$O_{\ell^2 q^2 g}^{(3)}$	$(\bar{\ell} \tau^i \gamma^\mu \ell)(\bar{q} \tau^i \gamma^\nu T^a q) G_{\mu\nu}^a$
$\tilde{O}_{e^2 u^2 g}$	$(\bar{e} \gamma^\mu e)(\bar{u} \gamma^\nu T^a u) \tilde{G}_{\mu\nu}^a$	$O_{e^2 u^2 g}$	$(\bar{e} \gamma^\mu e)(\bar{u} \gamma^\nu T^a u) G_{\mu\nu}^a$
$\tilde{O}_{e^2 d^2 g}$	$(\bar{e} \gamma^\mu e)(\bar{d} \gamma^\nu T^a d) \tilde{G}_{\mu\nu}^a$	$O_{e^2 d^2 g}$	$(\bar{e} \gamma^\mu e)(\bar{d} \gamma^\nu T^a d) G_{\mu\nu}^a$
$\tilde{O}_{\ell^2 u^2 g}$	$(\bar{\ell} \gamma^\mu \ell)(\bar{u} \gamma^\nu T^a u) \tilde{G}_{\mu\nu}^a$	$O_{\ell^2 u^2 g}$	$(\bar{\ell} \gamma^\mu \ell)(\bar{u} \gamma^\nu T^a u) G_{\mu\nu}^a$
$\tilde{O}_{\ell^2 d^2 g}$	$(\bar{\ell} \gamma^\mu \ell)(\bar{d} \gamma^\nu T^a d) \tilde{G}_{\mu\nu}^a$	$O_{\ell^2 d^2 g}$	$(\bar{\ell} \gamma^\mu \ell)(\bar{d} \gamma^\nu T^a d) G_{\mu\nu}^a$
$\tilde{O}_{q^2 e^2 g}$	$(\bar{e} \gamma^\mu e)(\bar{q} \gamma^\nu T^a q) \tilde{G}_{\mu\nu}^a$	$O_{q^2 e^2 g}$	$(\bar{e} \gamma^\mu e)(\bar{q} \gamma^\nu T^a q) G_{\mu\nu}^a$

# Standard Model Effective Field Theory

All SMEFT observables  $\mathcal{O}$  are linearized in SMEFT parameters.

XSection:

$$\sigma = F \int |\mathcal{A}|^2 d\text{LIPS} = \sigma_{\text{SM}} + \sum_k C_k \sigma_k$$

Asymmetry:

$$A = \text{ratio of polarized to unpolarized xsection} = A_{\text{SM}} + \sum_k C_k A_k$$

# Statistical analysis

A standard  $\chi^2$  test function:

$$\chi^2 = \sum_{bb'} (\mathcal{O} - \mathcal{O}^{(p)})_b \mathcal{H}_{bb'} (\mathcal{O} - \mathcal{O}^{(p)})_{b'}$$

$\mathcal{O}$ : SMEFT observable/model,  $\mathcal{O}^{(p)}$ : pseudodata,  $\mathcal{H}$ : inverse uncertainty matrix

$$\mathcal{O}_b^{(p)} = \mathcal{O}_b^{\text{SM}} + r_b \delta \mathcal{O}_b^{\text{uncorr}} + \sum_j r'_j \delta \mathcal{O}_b^{\text{corr}_j}, \quad r_b, r'_j \sim \mathcal{N}(0,1)$$

# Statistical analysis

A standard  $\chi^2$  test function:

$$\chi^2 = \sum_{bb'} (\mathcal{O} - \mathcal{O}^{(p)})_b \mathcal{H}_{bb'} (\mathcal{O} - \mathcal{O}^{(p)})_{b'}$$

$\mathcal{O}$ : SMEFT observable/model,  $\mathcal{O}^{(p)}$ : pseudodata,  $\mathcal{H}$ : inverse uncertainty matrix

$$\mathcal{O}_b^{(p)} = \mathcal{O}_b^{\text{SM}} + r_b \delta \mathcal{O}_b^{\text{uncorr}} + \sum_j r'_j \delta \mathcal{O}_b^{\text{corr}_j}, \quad r_b, r'_j \sim \mathcal{N}(0,1)$$

Various experimental uncertainty components:

EIC: statistical; uncorrelated systematic; fully correlated beam polarization or luminosity

LHeC/FCC-eh: statistical; global efficiency; fully correlated systematic (lepton energy and polar angle; hadron energy; radiative corrections; photoproduction background; calorimetry noise; luminosity)

HL-LHC: statistical

# Statistical analysis

A standard  $\chi^2$  test function:

$$\chi^2 = \sum_{bb'} (\mathcal{O} - \mathcal{O}^{(p)})_b \mathcal{H}_{bb'} (\mathcal{O} - \mathcal{O}^{(p)})_{b'}$$

$\mathcal{O}$ : SMEFT observable/model,  $\mathcal{O}^{(p)}$ : pseudodata,  $\mathcal{H}$ : inverse uncertainty matrix

$$\mathcal{O}_b^{(p)} = \mathcal{O}_b^{\text{SM}} + r_b \delta \mathcal{O}_b^{\text{uncorr}} + \sum_j r'_j \delta \mathcal{O}_b^{\text{corr}_j}, \quad r_b, r'_j \sim \mathcal{N}(0,1)$$

Best-fit values:

$$\nabla \chi^2(\hat{\mathbf{C}}) = 0$$

Fisher information matrix:

$$\mathcal{F} = \frac{1}{2} \nabla \nabla \chi^2(\hat{\mathbf{C}})$$

# Works



# Previously...

- Neutral-current parity-violating DIS asymmetries at EIC:

# Previously...

- Neutral-current parity-violating DIS asymmetries at EIC:
  - Semi-leptonic four-fermion operators  $O_{XY} = [\bar{\ell}\gamma^\mu P_X \ell][\bar{q}\gamma_\mu P_Y q]$

# Previously...

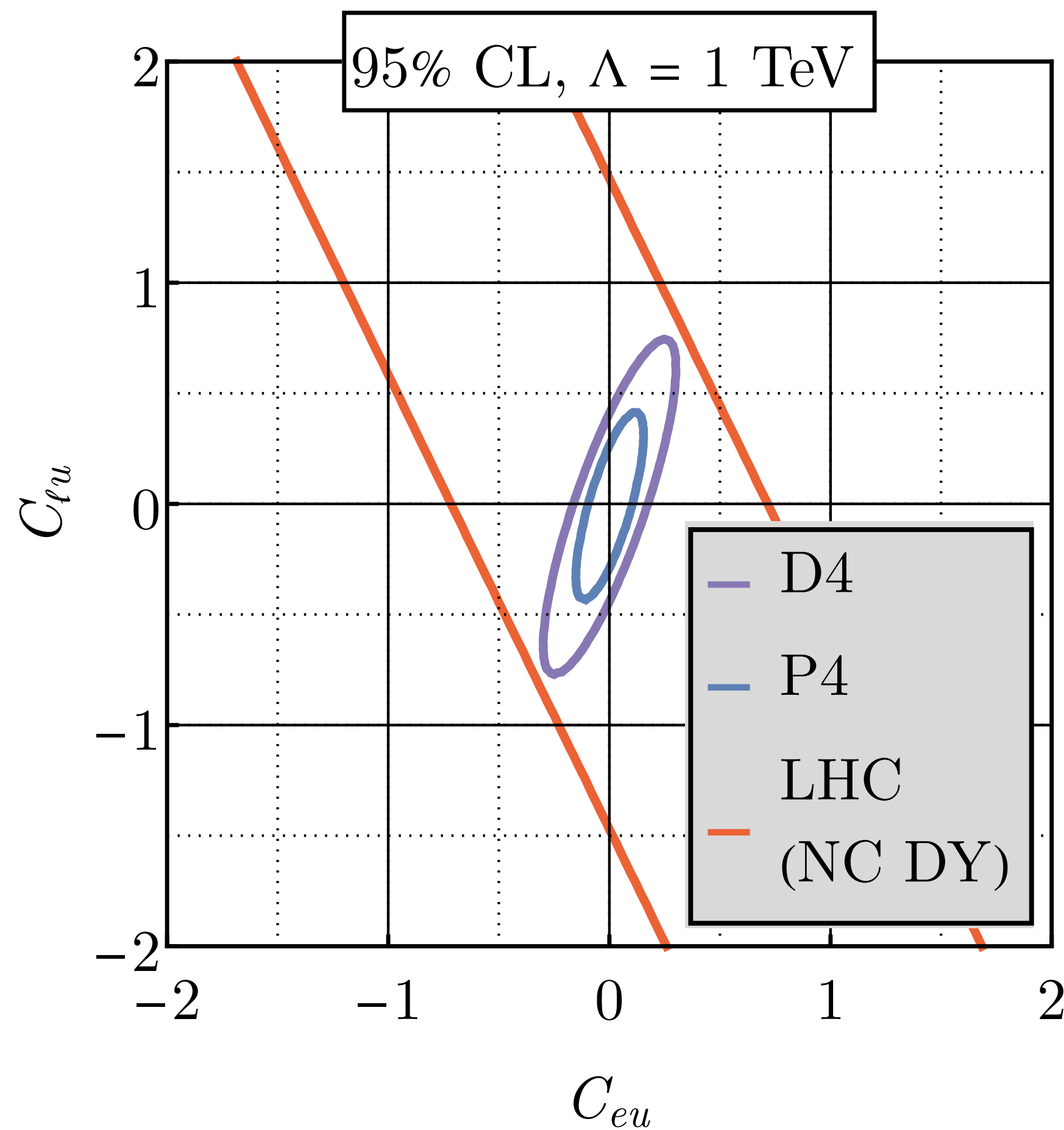
- Neutral-current parity-violating DIS asymmetries at EIC:
  - Semi-leptonic four-fermion operators  $O_{XY} = [\bar{\ell}\gamma^\mu P_X \ell][\bar{q}\gamma_\mu P_Y q]$
  - Simultaneous fits with beam polarization and luminosity difference parameters

# Previously...

- Neutral-current parity-violating DIS asymmetries at EIC:
  - Semi-leptonic four-fermion operators  $O_{XY} = [\bar{\ell}\gamma^\mu P_X \ell][\bar{q}\gamma_\mu P_Y q]$
  - Simultaneous fits with beam polarization and luminosity difference parameters
  - Resolve flat directions in neutral-current DY at the LHC

# Previously...

- Neutral-current parity-violating DIS asymmetries at EIC:



D4:  $10 \text{ GeV} \times 137 \text{ GeV } e^-D, 100 \text{ fb}^{-1}$

P4:  $10 \text{ GeV} \times 275 \text{ GeV } e^-p, 100 \text{ fb}^{-1}$

LHC:  $8 \text{ TeV}, 20 \text{ fb}^{-1}$ , not 13 TeV and HL, adapted  
from Boughezal+ [[2104.03979](#)]

# Previously...

- Neutral-current parity-violating DIS asymmetries at EIC:
  - Semi-leptonic four-fermion operators  $O_{XY} = [\bar{\ell}\gamma^\mu\ell][\bar{q}\gamma_\mu q]$
  - Simultaneous fits with beam polarization and luminosity difference parameters
  - Resolve flat directions in neutral-current DY at the LHC
  - Effective UV scales 1 to 4 TeV in single Wilson coefficient fits

# Previously...

- Neutral-current parity-violating DIS asymmetries at EIC + polarized xsection at LHeC and FCC-eh with NLO QCD corrections:

# Previously...

- Neutral-current parity-violating DIS asymmetries at EIC + polarized xsection at LHeC and FCC-eh with NLO QCD corrections:
  - Semi-leptonic four-fermion operators  $O_{XY} = [\bar{\ell}\gamma^\mu P_X \ell][\bar{q}\gamma_\mu P_Y q]$

# Previously...

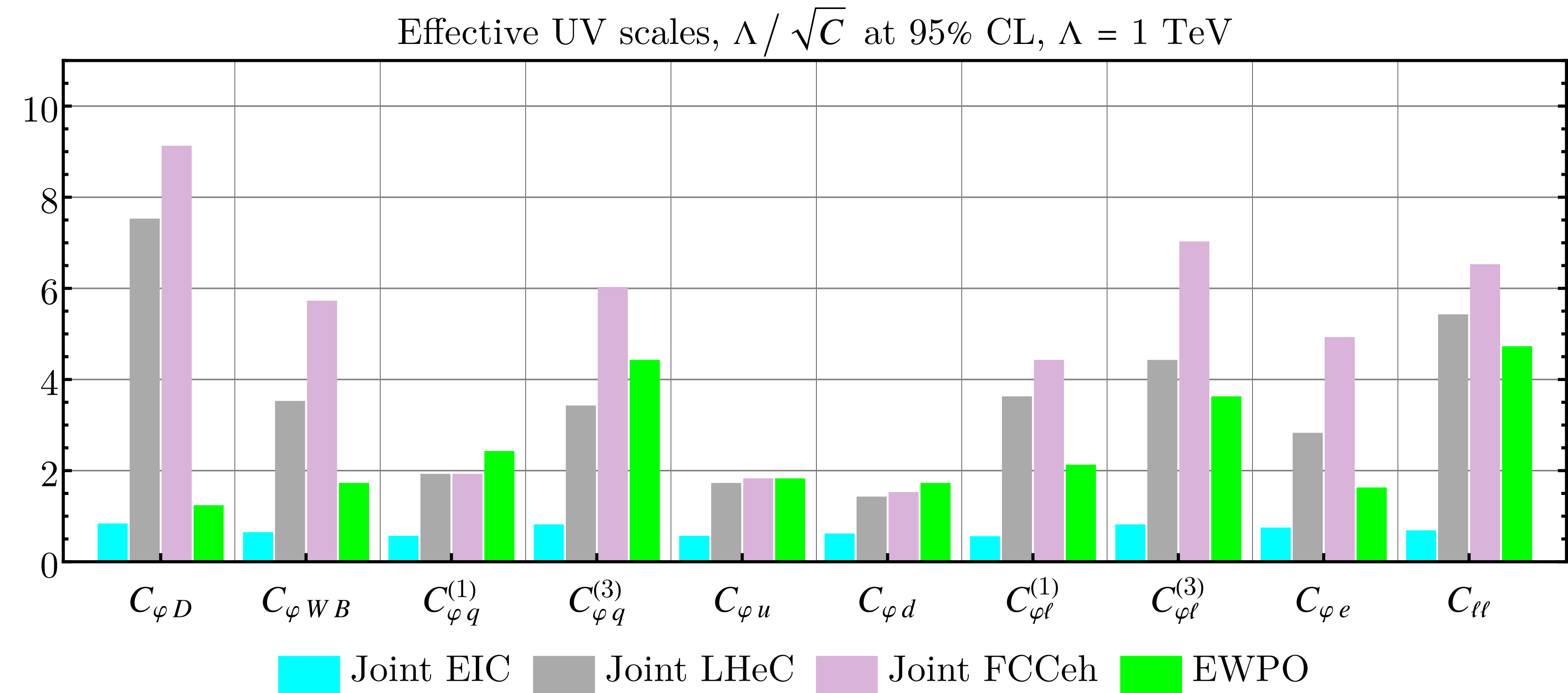
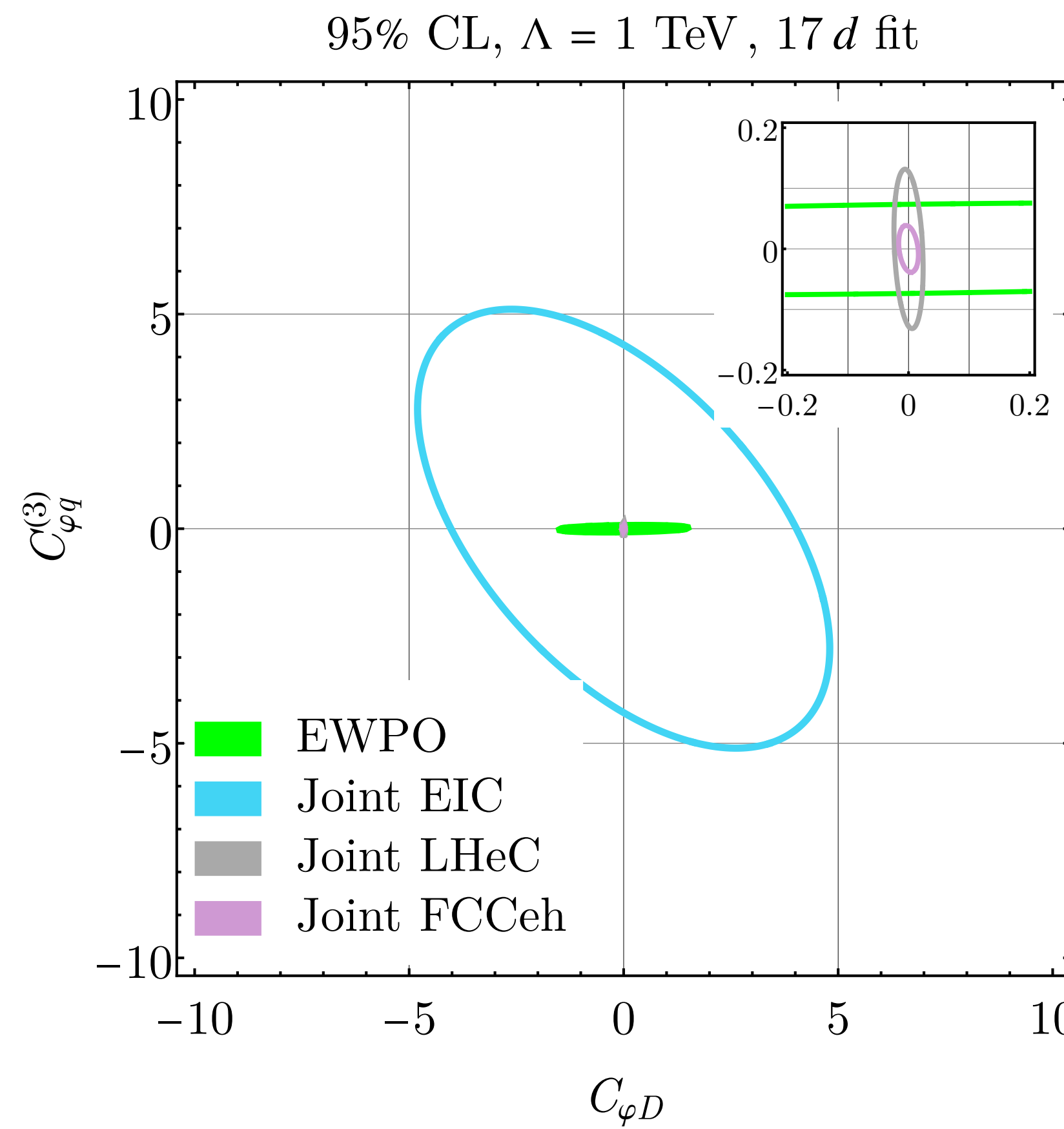
- Neutral-current parity-violating DIS asymmetries at EIC + polarized xsection at LHeC and FCC-eh with NLO QCD corrections:
  - Semi-leptonic four-fermion operators  $O_{XY} = [\bar{\ell}\gamma^\mu P_X \ell][\bar{q}\gamma_\mu P_Y q]$
  - Operators modifying  $ffV$  vertices

# Previously...

- Neutral-current parity-violating DIS asymmetries at EIC + polarized xsection at LHeC and FCC-eh with NLO QCD corrections:
  - Semi-leptonic four-fermion operators  $O_{XY} = [\bar{\ell}\gamma^\mu P_X \ell][\bar{q}\gamma_\mu P_Y q]$
  - Operators modifying  $ffV$  vertices
  - Resolve flat directions in global EWPO fits

# Previously...

- Neutral-current parity-violating DIS asymmetries at EIC + polarized xsection at LHeC and FCC-eh with NLO QCD corrections:



EWPO: 34d fit using Higgs, diboson, top data adapted from Ellis+ [[2012.02779](#)]

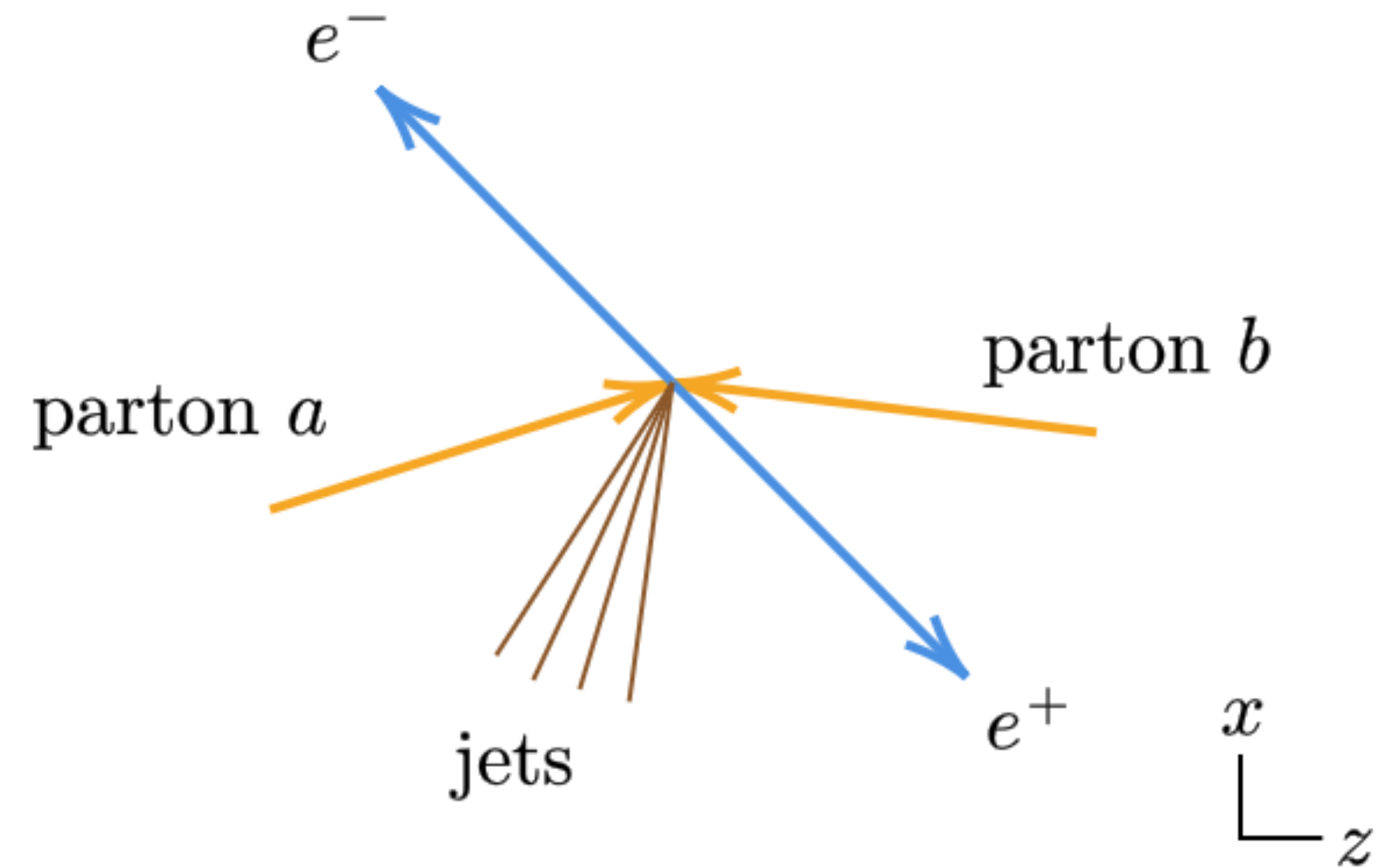
# Probing $CP$ -odd dimension-8 SMEFT with DYj at HL-LHC

# Probing $CP$ -odd dimension-8 SMEFT with DY $j$ at HL-LHC

- Angular distribution of  $pp \rightarrow je^-e^+$  encodes rich structure when written in Collins-Soper (CS) basis.
- The moments  $A_6$  and  $A_7$  are naive  $T$ -odd.
  - Vanish at tree level in SM
  - Activated at  $O(\alpha_s^2)$ , or with two or more jets at tree level
- SMEFT introduces operators that can generate  $CP$ -violating observables.
- No one has looked at this sector at HL-LHC; studies focus on inclusive DY.
- Goal: Use the clean null prediction for  $A_6$  and  $A_7$  in SM to probe new physics with high statistics.

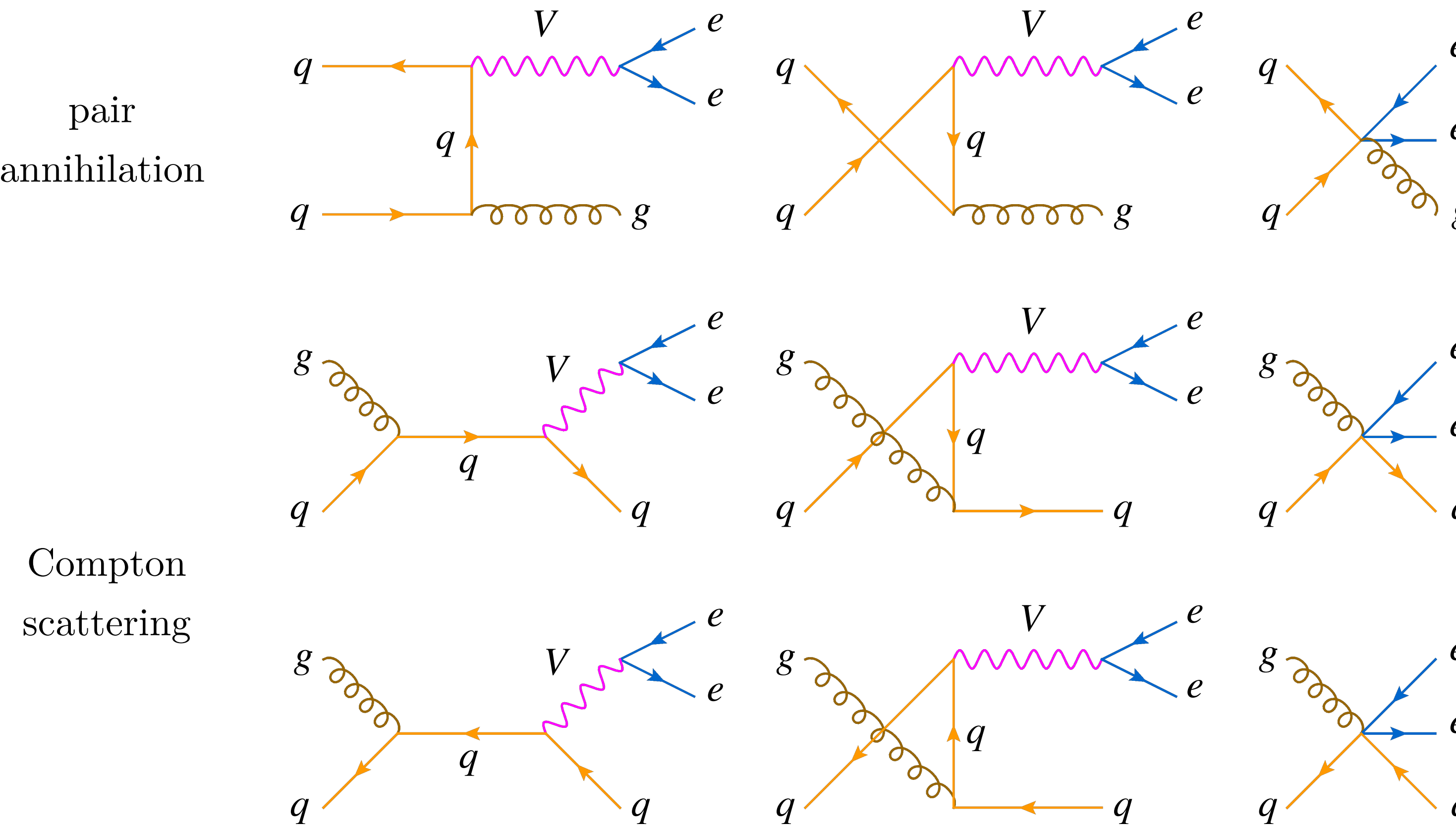
# Probing $CP$ -odd dimension-8 SMEFT with DY $j$ at HL-LHC

- Process of interest:  $pp \rightarrow j\gamma/Z^* \rightarrow je^-e^+$
- Jet enables construction of CS frame



# Probing $CP$ -odd dimension-8 SMEFT with $DYj$ at HL-LHC

- Process of interest:  $pp \rightarrow j\gamma/Z^* \rightarrow je^-e^+$



Semi-leptonic four-fermion operators coupled to gluon field strength tensor:

$$O_{XYg} = [\bar{\ell}\gamma^\mu P_X \ell][\bar{q}\gamma^\nu P_Y T^A q] G_{\mu\nu}^A$$

$$\tilde{O}_{XYg} = [\bar{\ell}\gamma^\mu P_X \ell][\bar{q}\gamma^\nu P_Y T^A q] \tilde{G}_{\mu\nu}^A$$

# Probing $CP$ -odd dimension-8 SMEFT with $DYj$ at HL-LHC

XSection in terms of CS moments:

$$\frac{d\sigma}{d\Omega^\star} = \frac{3\sigma}{16\pi} \left[ 1 + c_{\theta^\star}^2 + \sum_{m=0}^7 A_m Y_m(\Omega^\star) \right]$$

Angular structures:

$$Y_0 = \frac{1}{2}(1 - 3c_{\theta^\star}^2), \quad Y_1 = s_{2\theta^\star}c_{\varphi^\star}, \quad Y_2 = \frac{1}{2}s_{\theta^\star}^2c_{2\varphi^\star}, \quad Y_3 = s_{\theta^\star}c_{\varphi^\star}, \quad Y_4 = c_{\theta^\star},$$

$$Y_5 = s_{\theta^\star}^2s_{2\varphi^\star}, \quad Y_6 = s_{2\theta^\star}s_{\varphi^\star}, \quad Y_7 = s_{\theta^\star}s_{\varphi^\star}$$

CS moments:

$$A_0 = \frac{20}{3}\langle Y_0 \rangle + \frac{2}{3}, \quad A_1 = 5\langle Y_1 \rangle, \quad A_2 = 20\langle Y_2 \rangle, \quad A_3 = 4\langle Y_3 \rangle, \quad A_4 = 4\langle Y_4 \rangle,$$

$$A_5 = 5\langle Y_5 \rangle, \quad A_6 = 5\langle Y_6 \rangle, \quad A_7 = 4\langle Y_7 \rangle$$

$$Y_4 \propto Y_1^0$$

$$Y_7 \propto Y_1^1 + Y_1^{-1}$$

$$Y_3 \propto Y_1^1 - Y_1^{-1}$$

$$Y_0 \propto Y_2^0$$

$$Y_6 \propto Y_2^1 + Y_2^{-1}$$

$$Y_1 \propto Y_2^1 - Y_2^{-1}$$

$$Y_2 \propto Y_2^2 + Y_2^{-2}$$

$$Y_5 \propto Y_2^2 - Y_2^{-2}$$

$$\langle Y_m \rangle = \frac{\int Y_m d\sigma}{\sigma}$$

# Probing $CP$ -odd dimension-8 SMEFT with $DYj$ at HL-LHC

$\{\tilde{O}_{XYg}\}$ : studied with inclusive xsection (Boughezal+ [[2207.01703](#)]).

Focus on  $\{O_{XYg}\}$ .

# Probing $CP$ -odd dimension-8 SMEFT with $DYj$ at HL-LHC

$\{\tilde{O}_{XYg}\}$ : studied with inclusive xsection (Bouhezal+ [[2207.01703](#)]).

Focus on  $\{O_{XYg}\}$ .

Observables:  $A_6$  and  $A_7$

- $A_0$  through  $A_4$  are proportional to  $\Gamma_Z \Rightarrow$  vanish at high end tail
- $A_5$  doesn't require  $\Gamma_Z$  but shows strong cancellations due to kinematics

# Probing $CP$ -odd dimension-8 SMEFT with DY $j$ at HL-LHC

$\{\tilde{O}_{XYg}\}$ : studied with inclusive xsection (Boughezal+ [[2207.01703](#)]).

Focus on  $\{O_{XYg}\}$ .

Observables:  $A_6$  and  $A_7$

- $A_0$  through  $A_4$  are proportional to  $\Gamma_Z \Rightarrow$  vanish at high end tail
- $A_5$  doesn't require  $\Gamma_Z$  but shows strong cancellations due to kinematics

Observables are linearized:

$$A = N\langle Y \rangle = N \frac{\int Y d\sigma}{\sigma} = \frac{N_{\text{SM}} + \sum_k C_k N_k}{D_{\text{SM}} + \sum_k C_k D_k} = A_{\text{SM}} + \sum_k C_k A_k$$

# Probing $CP$ -odd dimension-8 SMEFT with $DYj$ at HL-LHC

$\{\tilde{O}_{XYg}\}$ : studied with inclusive xsection (Boughezal+ [[2207.01703](#)]).

Focus on  $\{O_{XYg}\}$ .

Observables:  $A_6$  and  $A_7$

- $A_0$  through  $A_4$  are proportional to  $\Gamma_Z \Rightarrow$  vanish at high end tail
- $A_5$  doesn't require  $\Gamma_Z$  but shows strong cancellations due to kinematics

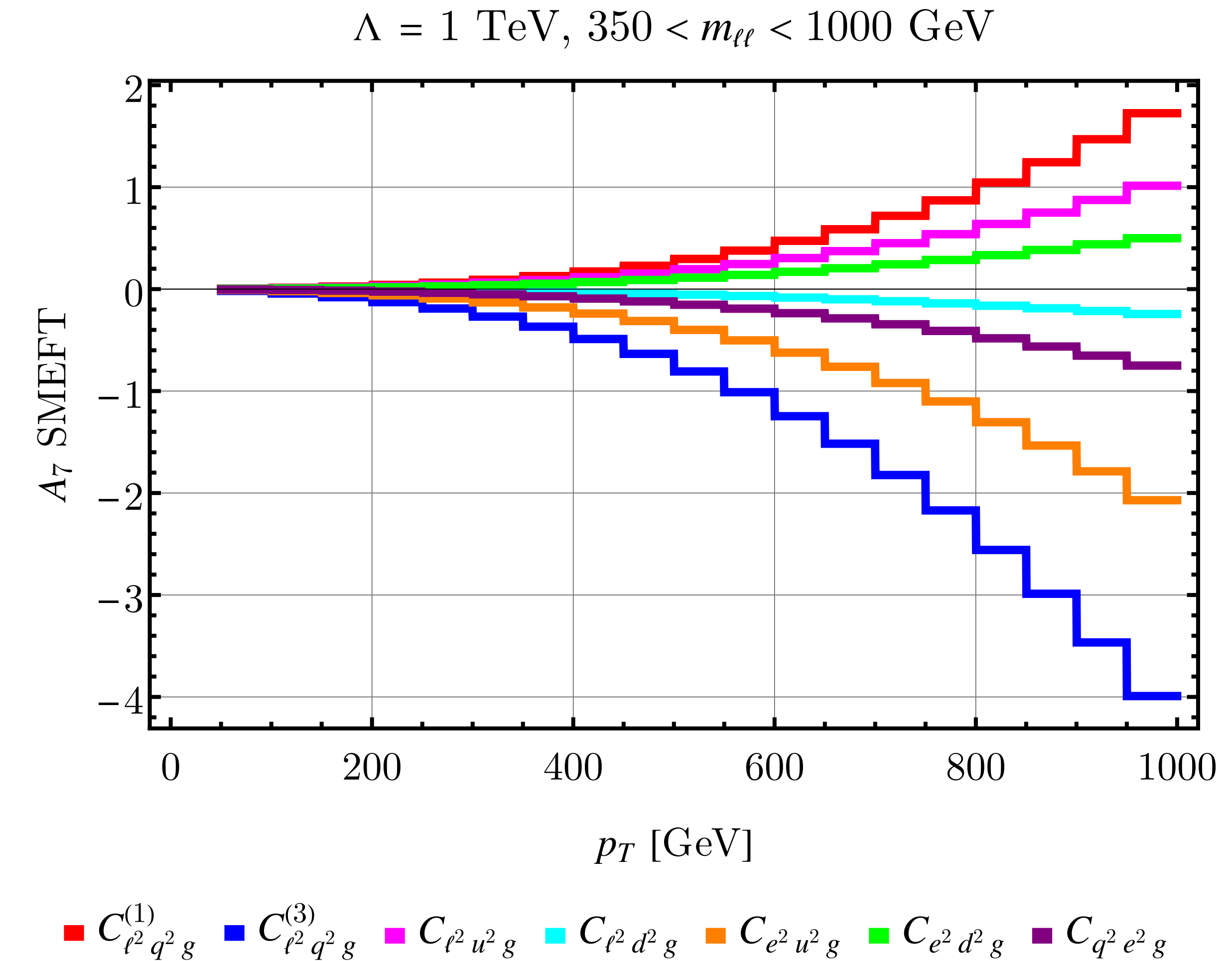
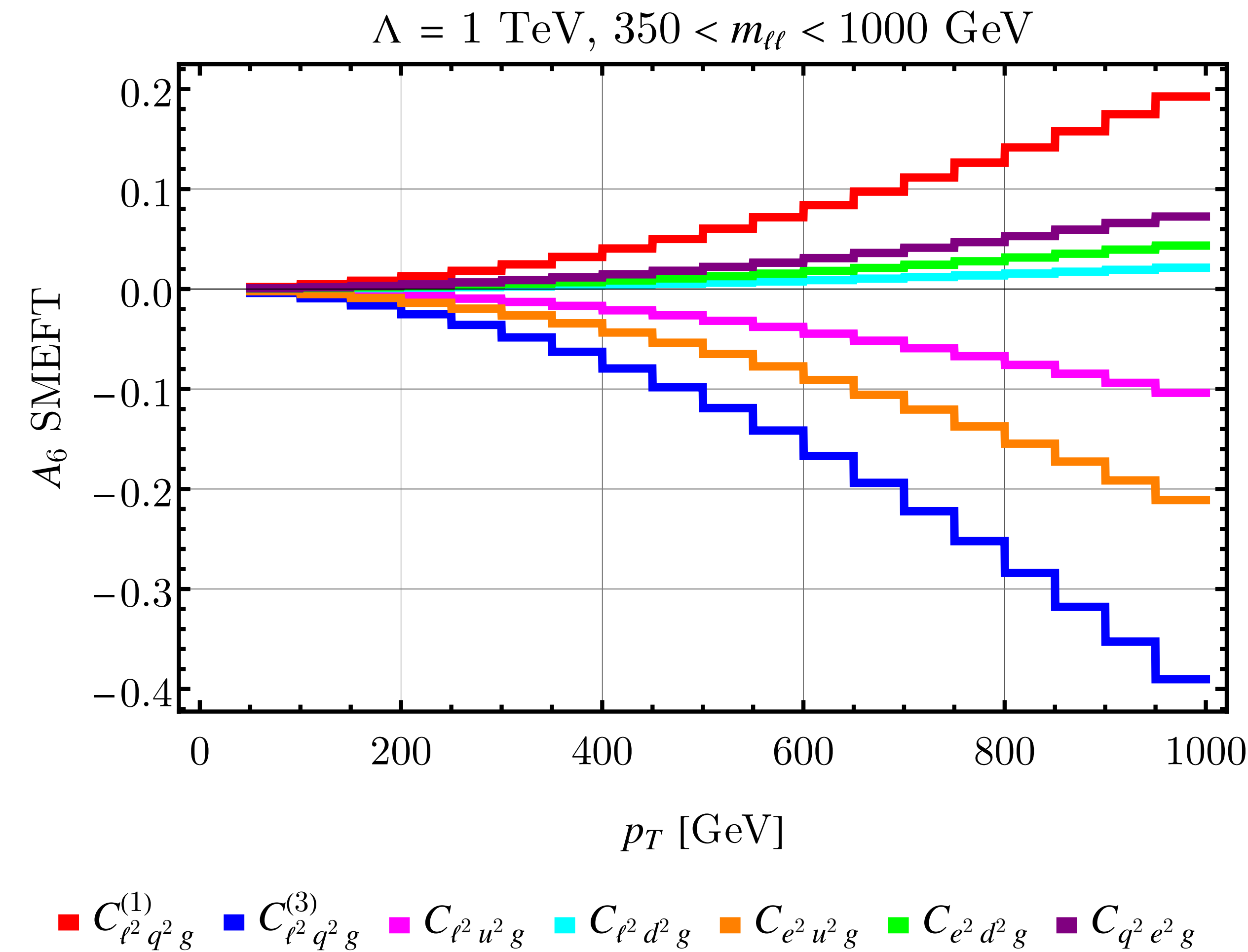
Observables are linearized:

$$A = N\langle Y \rangle = N \frac{\int Y d\sigma}{\sigma} = \frac{N_{\text{SM}} + \sum_k C_k N_k}{D_{\text{SM}} + \sum_k C_k D_k} = A_{\text{SM}}^0 + \sum_k C_k A_k$$

0

↑

# Probing $CP$ -odd dimension-8 SMEFT with $DYj$ at HL-LHC



# Probing $CP$ -odd dimension-8 SMEFT with DY $j$ at HL-LHC

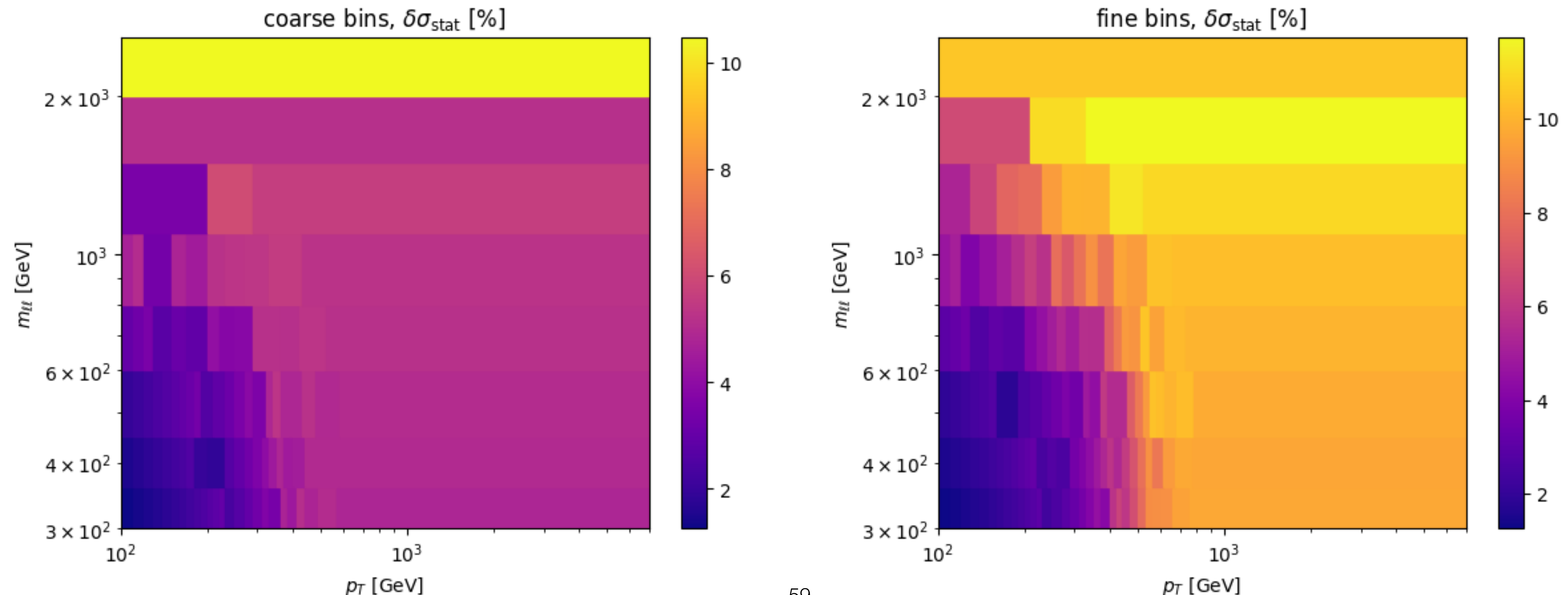
HL-LHC simulation:  $\sqrt{s} = 14$  TeV,  $L = 3$  ab $^{-1}$

Detector cuts:

- Leading electron:  $p_T > 25$  GeV, subleading electron  $p_T > 20$  GeV
- Both electrons:  $|\eta| < 2.4$
- Jet:  $p_T > 30$  GeV,  $|y| > 2.4$
- Jet-electron separation:  $\Delta R_{je} > 0.4$  for all jet-electron pairs
- Dilepton system:  $p_T > 100$  GeV,  $|y| < 2.4$

# Probing $CP$ -odd dimension-8 SMEFT with $DYj$ at HL-LHC

Coarse and fine bins:  $300 < m_{\ell\ell} < 2600$  GeV,  $100 < p_T < 7000$  GeV



# Probing $CP$ -odd dimension-8 SMEFT with DY $j$ at HL-LHC

Experimental uncertainties:

- Statistical uncertainties:  $\delta A_m = \frac{N_m}{\sqrt{N}} \sqrt{\langle Y_m^2 \rangle}$ ,  $N = \sigma L$ ,  $\langle Y_m^2 \rangle = \frac{\int Y_m^2 d\sigma}{\sigma}$ ,  $m = 6, 7$

# Probing $CP$ -odd dimension-8 SMEFT with DY $j$ at HL-LHC

Experimental uncertainties:

- Statistical uncertainties:  $\delta A_m = \frac{N_m}{\sqrt{N}} \sqrt{\langle Y_m^2 \rangle}$ ,  $N = \sigma L$ ,  $\langle Y_m^2 \rangle = \frac{\int Y_m^2 d\sigma}{\sigma}$ ,  $m = 6, 7$
- Any relative uncertainty in  $\sigma \Rightarrow$  relative uncertainty in  $A_m \Rightarrow 0$

# Probing $CP$ -odd dimension-8 SMEFT with DY $j$ at HL-LHC

Experimental uncertainties:

- Statistical uncertainties:  $\delta A_m = \frac{N_m}{\sqrt{N}} \sqrt{\langle Y_m^2 \rangle}$ ,  $N = \sigma L$ ,  $\langle Y_m^2 \rangle = \frac{\int Y_m^2 d\sigma}{\sigma}$ ,  $m = 6, 7$
- Any relative uncertainty in  $\sigma \Rightarrow$  relative uncertainty in  $A_m \Rightarrow 0$

Theoretical uncertainties:

- PDF variations: Based on SM value of xsection  $\Rightarrow 0$

# Probing $CP$ -odd dimension-8 SMEFT with DY $j$ at HL-LHC

Experimental uncertainties:

- Statistical uncertainties:  $\delta A_m = \frac{N_m}{\sqrt{N}} \sqrt{\langle Y_m^2 \rangle}$ ,  $N = \sigma L$ ,  $\langle Y_m^2 \rangle = \frac{\int Y_m^2 d\sigma}{\sigma}$ ,  $m = 6, 7$
- Any relative uncertainty in  $\sigma \Rightarrow$  relative uncertainty in  $A_m \Rightarrow 0$

Theoretical uncertainties:

- PDF variations: Based on SM value of xsection  $\Rightarrow 0$
- Scale variations: Based on SM value of xsection  $\Rightarrow 0$

# Probing $CP$ -odd dimension-8 SMEFT with $DYj$ at HL-LHC

Experimental uncertainties:

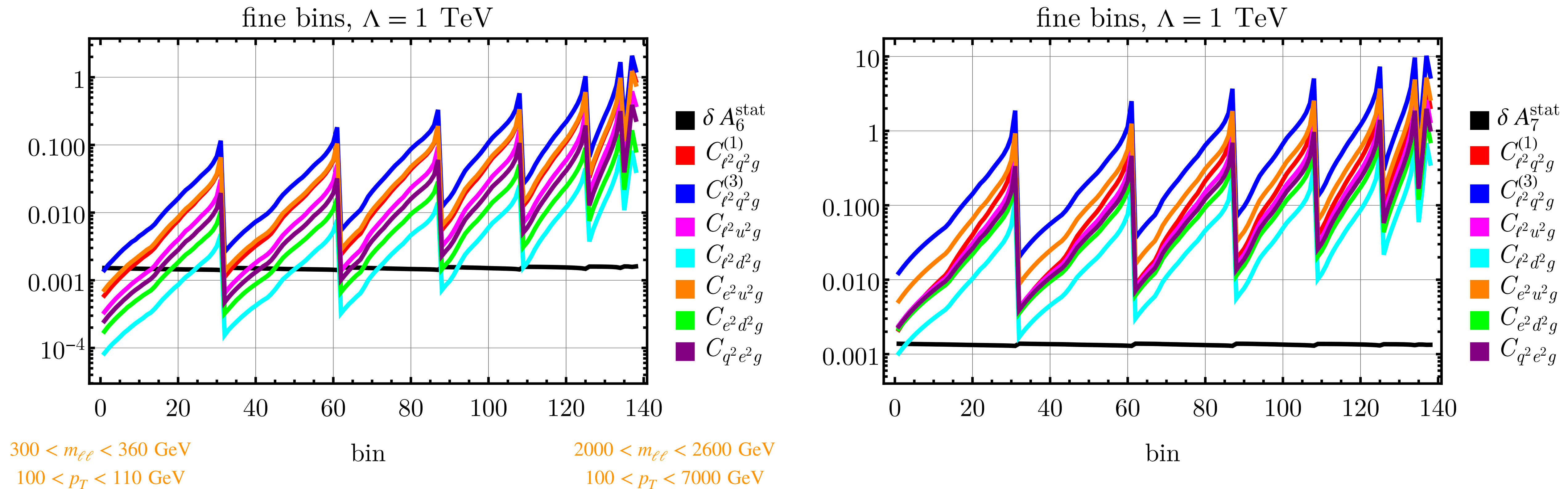
- Statistical uncertainties:  $\delta A_m = \frac{N_m}{\sqrt{N}} \sqrt{\langle Y_m^2 \rangle}$ ,  $N = \sigma L$ ,  $\langle Y_m^2 \rangle = \frac{\int Y_m^2 d\sigma}{\sigma}$ ,  $m = 6, 7$
- Any relative uncertainty in  $\sigma \Rightarrow$  relative uncertainty in  $A_m \Rightarrow 0$

Theoretical uncertainties:

- PDF variations: Based on SM value of xsection  $\Rightarrow 0$
  - Scale variations: Based on SM value of xsection  $\Rightarrow 0$
- $\therefore$  We have only statistical uncertainties.

# Probing $CP$ -odd dimension-8 SMEFT with $DYj$ at HL-LHC

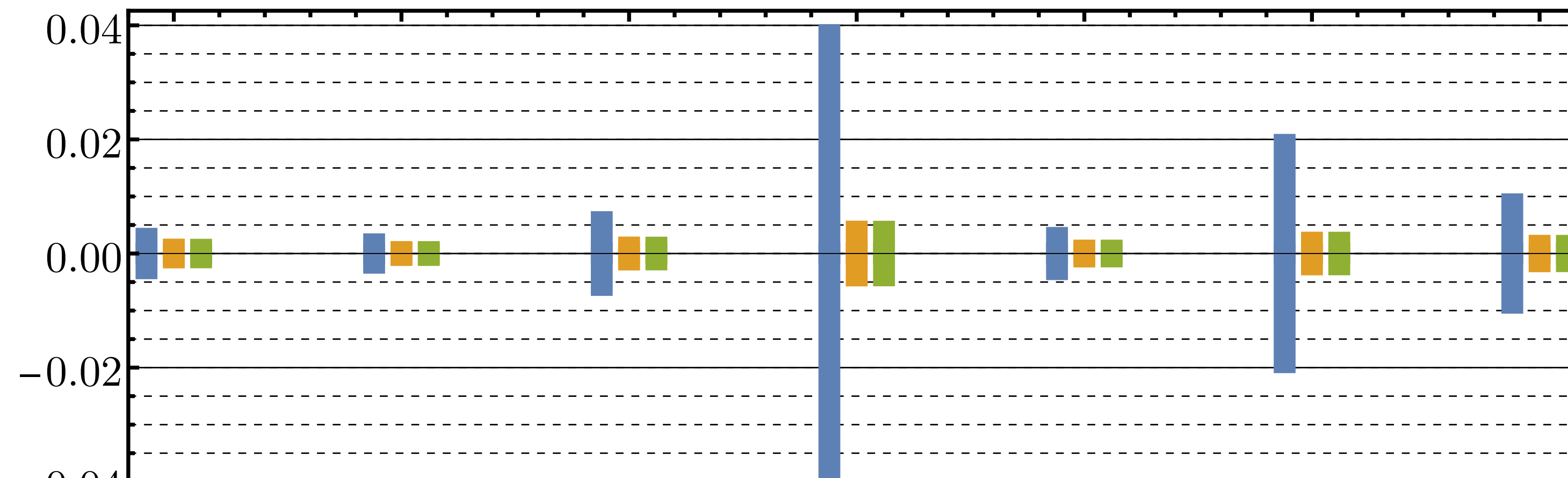
Error budget:



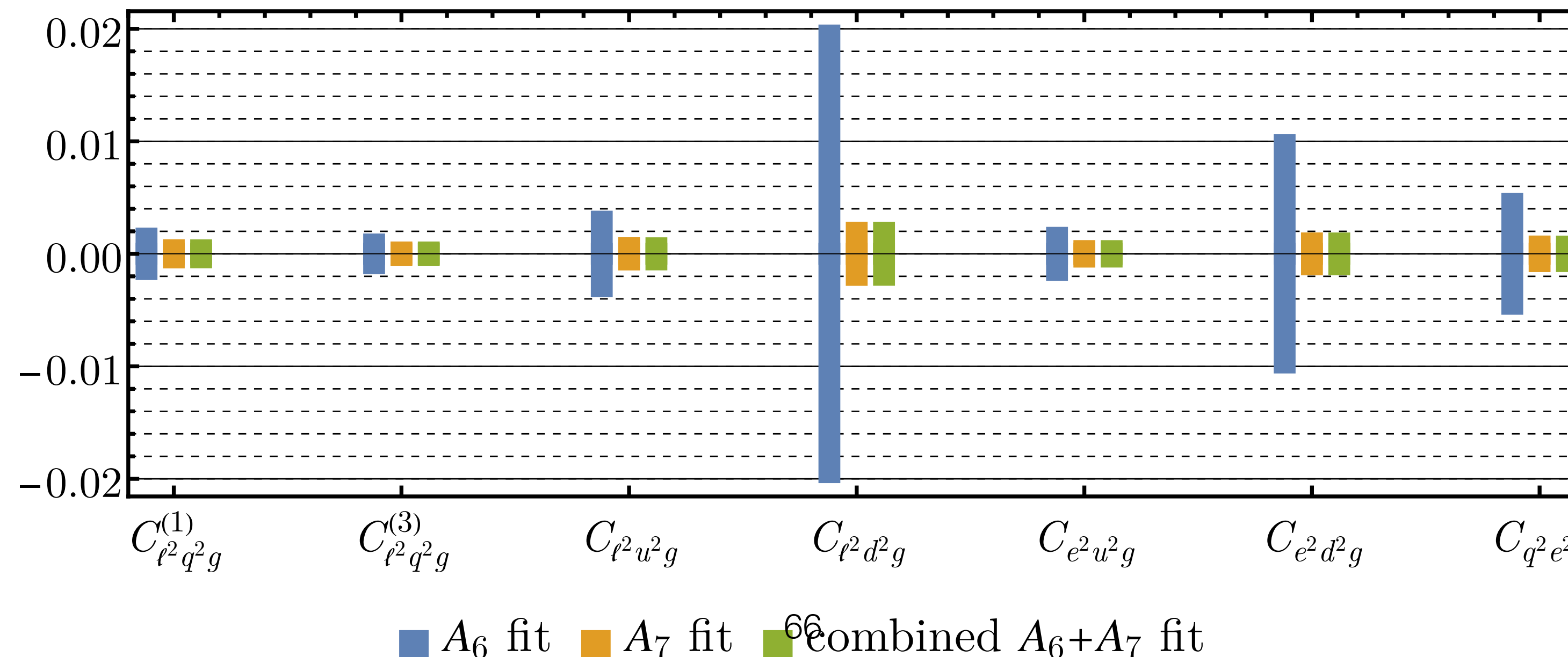
Bins are sorted by  $m_{\ell\ell}$  first and then by  $p_T$ .

# Probing $CP$ -odd dimension-8 SMEFT with $DYj$ at HL-LHC

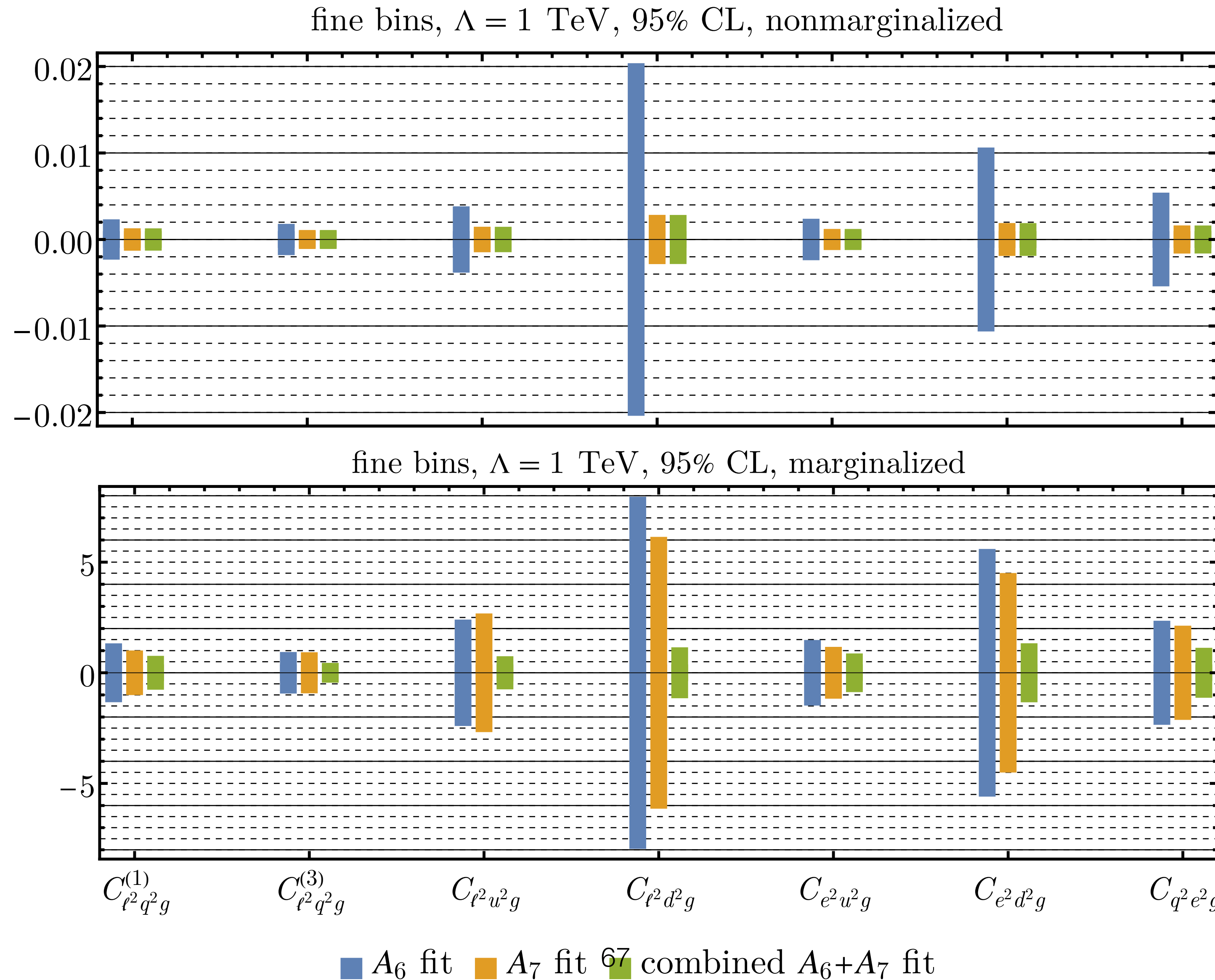
coarse bins,  $\Lambda = 1$  TeV, 95% CL, nonmarginalized



fine bins,  $\Lambda = 1$  TeV, 95% CL, nonmarginalized

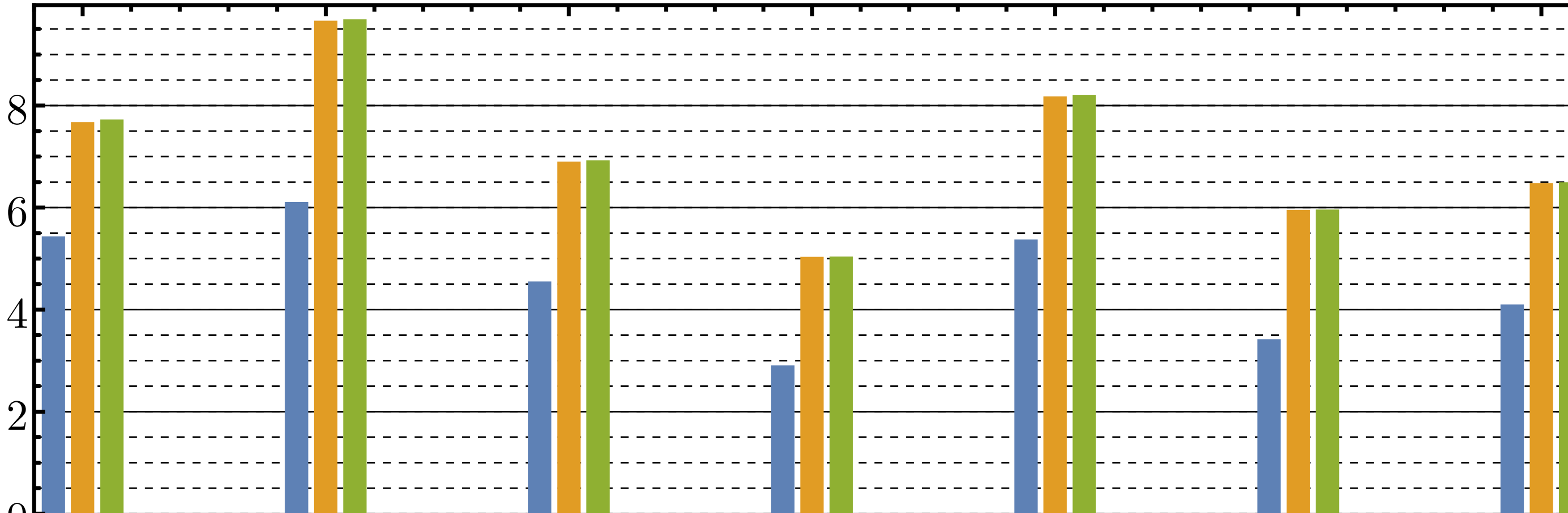


# Probing $CP$ -odd dimension-8 SMEFT with $DYj$ at HL-LHC

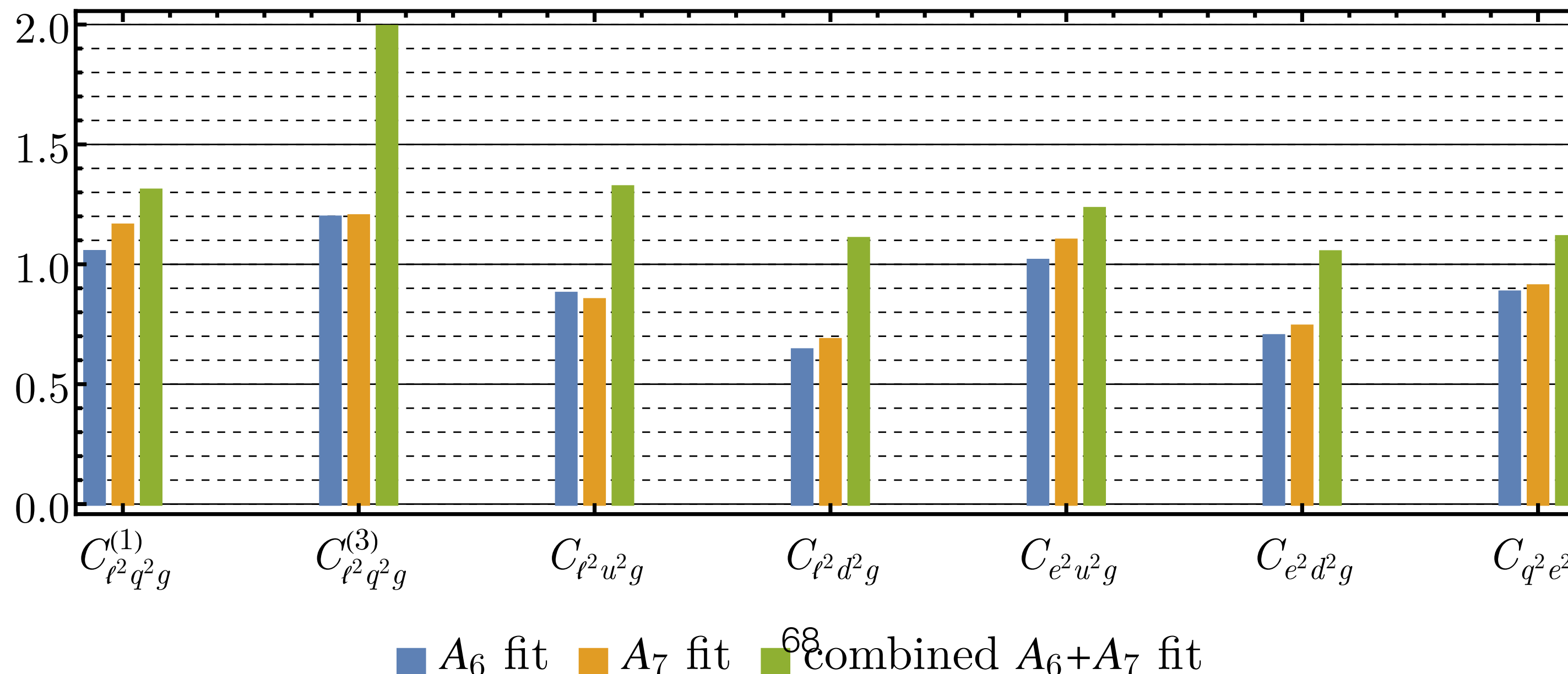


# Probing $CP$ -odd dimension-8 SMEFT with $DYj$ at HL-LHC

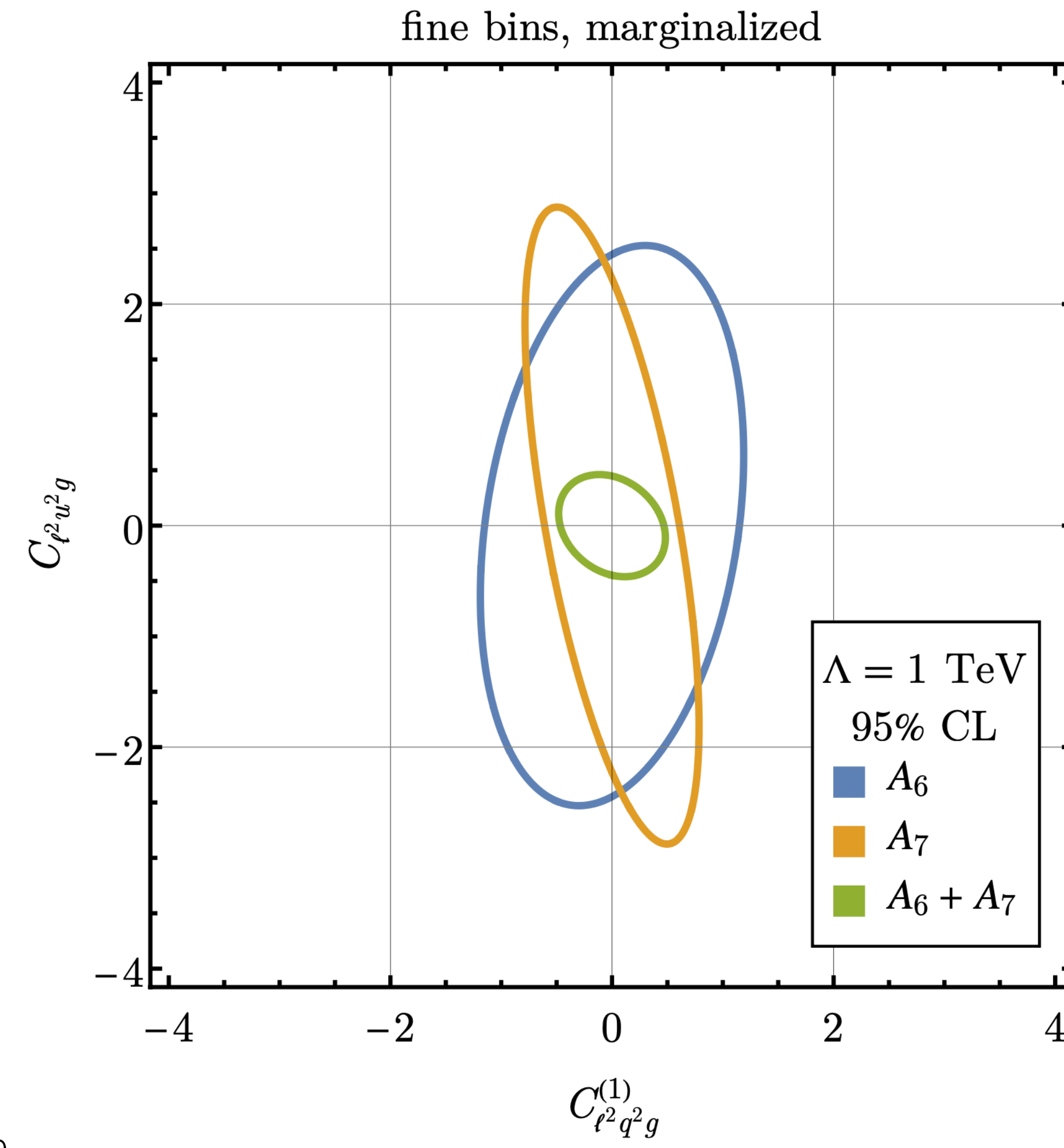
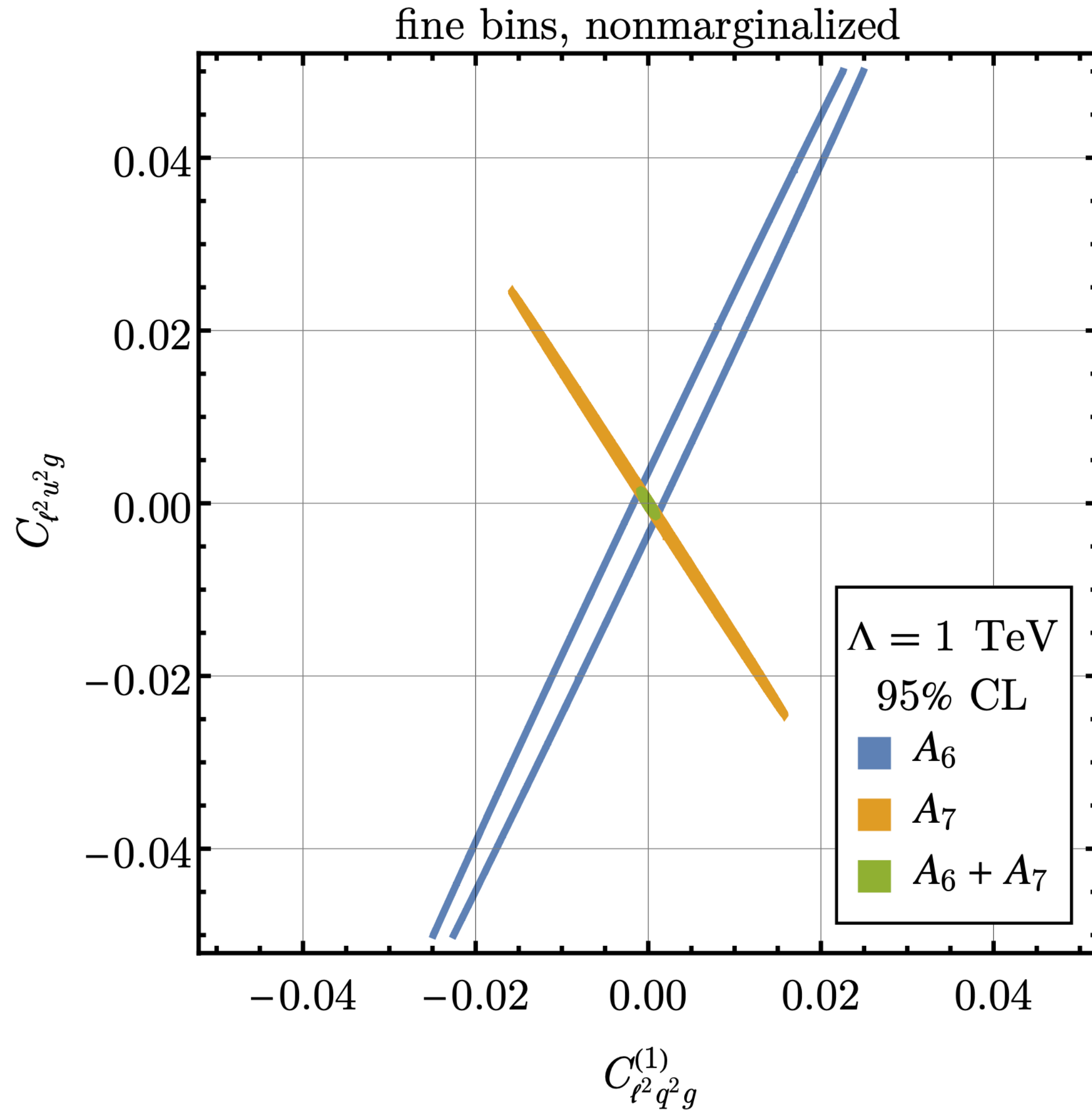
fine bins,  $\Lambda = 1$  TeV,  $\Lambda/C_w^{1/4}$  [TeV], 95% CL, nonmarginalized



fine bins,  $\Lambda = 1$  TeV,  $\Lambda/C_w^{1/4}$  [TeV], 95% CL, marginalized



# Probing $CP$ -odd dimension-8 SMEFT with $DYj$ at HL-LHC



# Probing $CP$ -odd dimension-8 SMEFT with $DYj$ at HL-LHC

Previously unexplored sector of dimension-8 SMEFT:

- Tight bounds  $\Rightarrow \Lambda_{\text{eff}} \sim 9$  TeV in single-parameter fits
- Bounds weakened by two orders  $\Rightarrow$  strong correlations

# Probing $CP$ -odd dimension-8 SMEFT with $DYj$ at HL-LHC

Previously unexplored sector of dimension-8 SMEFT:

- Tight bounds  $\Rightarrow \Lambda_{\text{eff}} \sim 9$  TeV in single-parameter fits
- Bounds weakened by two orders  $\Rightarrow$  strong correlations

Future plans for this work:

- UV matching
- New operators

# Probing $y_e$ via transverse spin asymmetries at the FCC-ee

# Probing $y_e$ via transverse spin asymmetries at the FCC-ee

- Electron Yukawa coupling,  $y_e^{\text{SM}} = \frac{\sqrt{2}m_e}{v} \approx 2.9 \times 10^{-9}$ , the tiniest in SM
- Measuring this = one of the most precise tests

# Probing $y_e$ via transverse spin asymmetries at the FCC-ee

- Electron Yukawa coupling,  $y_e^{\text{SM}} = \frac{\sqrt{2}m_e}{v} \approx 2.9 \times 10^{-9}$ , the tiniest in SM
- Measuring this = one of the most precise tests
- Bounds from DY at LHC:  $|y_e| \leq 260 |y_e^{\text{SM}}|$  at  $2\sigma$
- Projected bounds from HL-LHC:  $|y_e| \geq 120 |y_e^{\text{SM}}|$
- Challenging because xsection  $\propto y_e^2$

# Probing $y_e$ via transverse spin asymmetries at the FCC-ee

- More direct access at FCC-ee near Higgs resonance,  $\sqrt{s} = 125$  GeV
- Most complete analysis of inclusive xsection:  $|y_e| \leq 1.6 |y_e^{\text{SM}}|$  (d'Enterria+ [[2107.02686](#)])

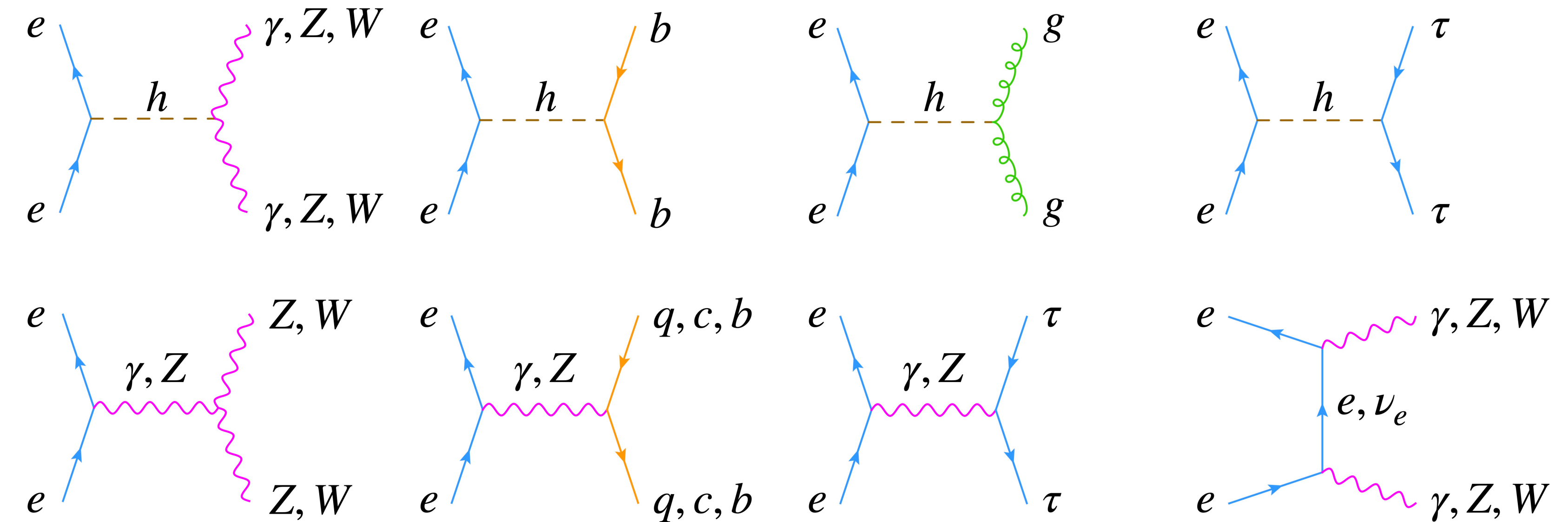
# Probing $y_e$ via transverse spin asymmetries at the FCC-ee

- More direct access at FCC-ee near Higgs resonance,  $\sqrt{s} = 125$  GeV
- Most complete analysis of inclusive xsection:  $|y_e| \leq 1.6 |y_e^{\text{SM}}|$  (d'Enterria+ [[2107.02686](#)])  
**can't escape  $y_e^2$  suppression!**

# Probing $y_e$ via transverse spin asymmetries at the FCC-ee

- More direct access at FCC-ee near Higgs resonance,  $\sqrt{s} = 125$  GeV
- Most complete analysis of inclusive xsection:  $|y_e| \leq 1.6 |y_e^{\text{SM}}|$  (d'Enterria+ [[2107.02686](#)])  
can't escape  $y_e^2$  suppression!

large EW continuum background!



# Probing $y_e$ via transverse spin asymmetries at the FCC-ee

- A new avenue: transverse spin asymmetries
  - Chiral mass suppression: still an obstacle
  - Arise from Higgs-background interference  $\therefore$  linear  $y_e$  suppression
  - With a proper weight  $\Rightarrow$  can isolate signal from background

# Probing $y_e$ via transverse spin asymmetries at the FCC-ee

- A new avenue: transverse spin asymmetries
  - Chiral mass suppression: still an obstacle
  - Arise from Higgs-background interference  $\therefore$  linear  $y_e$  suppression
  - With a proper weight  $\Rightarrow$  can isolate signal from background
- Processes of interest:

$$e^+ e^- \rightarrow b\bar{b}$$

highest branching ratios

$$e^+ e^- \rightarrow WW \rightarrow \ell\nu jj$$

in  $e^+ e^- \rightarrow h$

# Probing $y_e$ via transverse spin asymmetries at the FCC-ee

- A new avenue: transverse spin asymmetries
  - Chiral mass suppression: still an obstacle
  - Arise from Higgs-background interference  $\therefore$  linear  $y_e$  suppression
  - With a proper weight  $\Rightarrow$  can isolate signal from background
- Processes of interest:

$$e^+e^- \rightarrow b\bar{b}$$

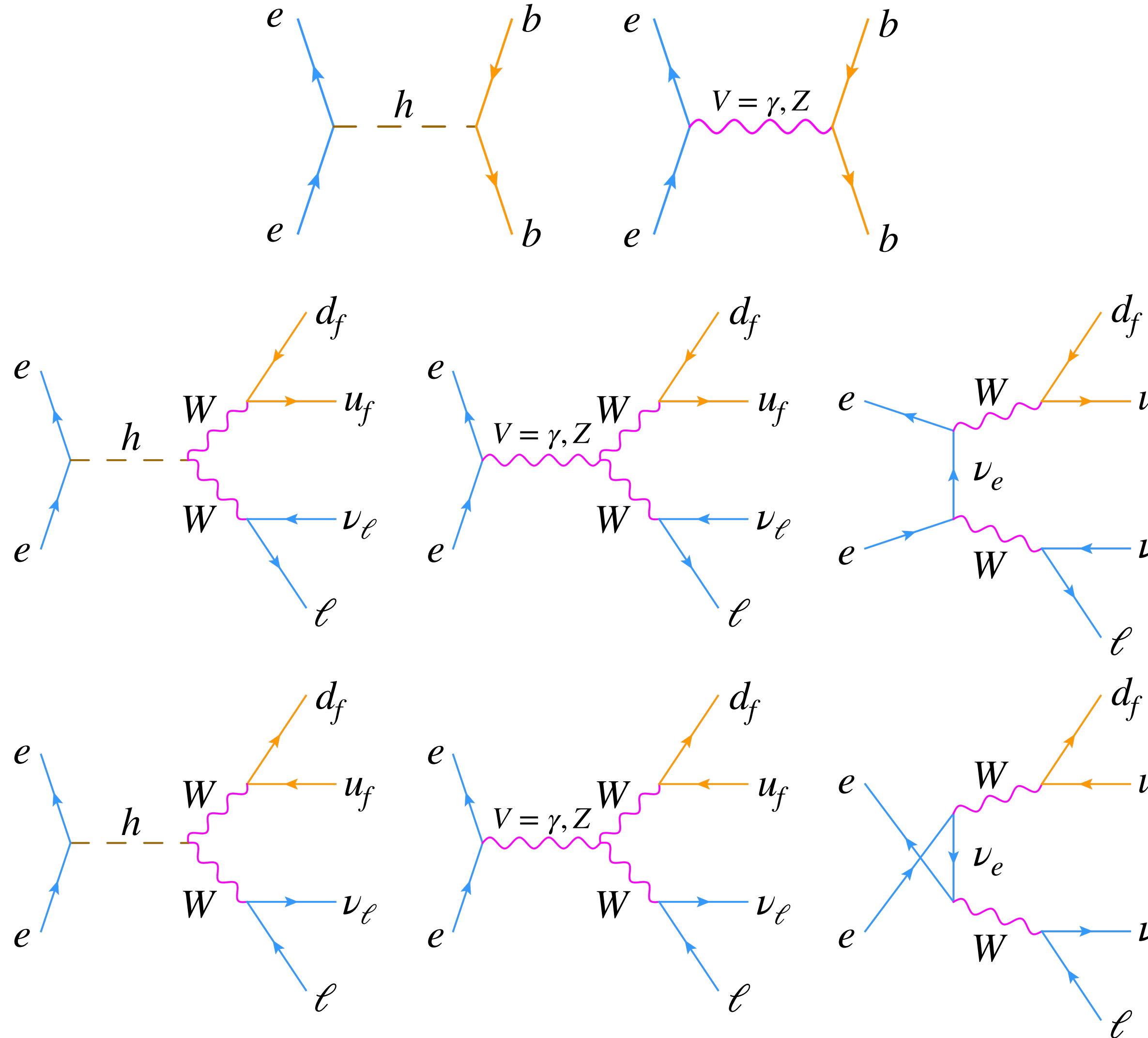
highest branching ratios

$$e^+e^- \rightarrow WW \rightarrow \ell\nu jj$$

in  $e^+e^- \rightarrow h$

- Construct asymmetry observables and assess statistical significance.
- Realistic experimental effects: beam energy spread, initial state radiation, optimized kinematic cuts

# Probing $y_e$ via transverse spin asymmetries at the FCC-ee



$$\sigma^{\lambda\bar{\lambda}} = F \int |\mathcal{A}^{\lambda\bar{\lambda}}|^2 \, d\text{LIPS}$$

electron: transverse polarization  
 positron: longitudinal polarization

$$u_\lambda \bar{u}_\lambda = (\gamma \cdot p + m) \mathbb{P}_\lambda^+(S_T)$$

$$v_\lambda \bar{v}_\lambda = (\gamma \cdot p - m) \mathbb{P}_\lambda^-(S_L)$$

$$S_T^\mu = (0, \cos(\varphi), \sin(\varphi), 0)$$

$$S_L^\mu = \frac{1}{m}(|\vec{p}|, E\hat{p})$$

# Probing $y_e$ via transverse spin asymmetries at the FCC-ee

Asymmetry observables:  $A = \frac{N}{D}$

$$N = \frac{1}{4}(\sigma^{++} - \sigma^{+-} - \sigma^{-+} + \sigma^{--}): \text{double polarization (DP)}$$

$$N = \frac{1}{2}(\sigma^{+0} - \sigma^{-0}): \text{single polarization with unpolarized positron (SP}^0\text{)}$$

$$N = \frac{1}{2}(\sigma^{++} - \sigma^{-+}): \text{single polarization with LH positron (SP}^+\text{)}$$

$$N = \frac{1}{2}(\sigma^{+-} - \sigma^{--}): \text{single polarization with RH positron (SP}^-\text{)}$$

$D$ : same as  $N$  with all the contributions added

# Probing $y_e$ via transverse spin asymmetries at the FCC-ee

Asymmetry observables:  $A = \frac{N}{D}$

$$N = \sum_c F \int w N^c \text{ dLIPS},$$

$c$ : channels ( $h, \gamma, Z, \nu, h\gamma, hZ, h\nu, \gamma Z, \gamma \nu, Z\nu$ )

$w$ : angular weight to eliminate interference channels, isolate  $y_e$

# Probing $y_e$ via transverse spin asymmetries at the FCC-ee

Asymmetry observables:  $A = \frac{N}{D}$

$$N = \sum_c F \int w N^c \text{ dLIPS},$$

$c$ : channels ( $h, \gamma, Z, \nu, h\gamma, hZ, h\nu, \gamma Z, \gamma \nu, Z\nu$ )

$w$ : angular weight to eliminate interference channels, isolate  $y_e$

Best angular weight:

$$w = \sin(\varphi)$$

$\varphi$ : azimuthal angle of  $b$  or  $W(\ell\nu)$  in the c.m. frame of  $e^+e^-$

Completely isolates  $y_e$  in  $b\bar{b}$ , maximally isolates in  $WW$  in  $hZ$  interference.

# Probing $y_e$ via transverse spin asymmetries at the FCC-ee

Dilution of the signal:

$$\sigma(E_{\text{coll}}) = \int_{-\infty}^{\infty} d\hat{E} \frac{dL(E_{\text{coll}}, \hat{E}, \delta)}{d\hat{E}} \int_0^1 dx f(x, \hat{E}) \sigma(\sqrt{x}\hat{E})$$

$$E_{\text{coll}} = m_h$$

$$\delta = \Gamma_h$$

$$\frac{dL(E_{\text{coll}}, \hat{E}, \delta)}{d\hat{E}} = \frac{1}{\sqrt{2\pi\delta^2}} \exp \left[ -\frac{(\hat{E} - E_{\text{coll}})^2}{2\delta^2} \right]$$

$f(x, \hat{E})$ : JWW ISR function

# Probing $y_e$ via transverse spin asymmetries at the FCC-ee

Sensitivity estimates:

$$A^{\text{exp}} = \frac{1}{P_{e^-} - P_{e^+}} \frac{N_N}{N_D}$$
: experimental reconstruction of asymmetry

$$N_N = \eta L N, \quad N_D = \eta L D$$
: event counts

$$\delta A^{\text{exp}} = \frac{\delta P_{e^-}}{P_{e^-}} A^{\text{exp}} \oplus \frac{\delta P_{e^+}}{P_{e^+}} A^{\text{exp}} \oplus \frac{1}{P_{e^-} - P_{e^+}} \frac{1}{\sqrt{N_D}}$$

$$P_{e^-} = 80\%, \quad P_{e^+} = 30\%, \quad 3\% \text{ relative uncertainties,}$$

$$L = 10 \text{ ab}^{-1}, \quad \eta = 80\% \text{ (100\%) for } b\bar{b} \text{ (WW)}$$

# Probing $y_e$ via transverse spin asymmetries at the FCC-ee

Sensitivity estimates:

$$A^{\text{exp}} = \frac{1}{P_{e^-} - P_{e^+}} \frac{N_N}{N_D}$$
: experimental reconstruction of asymmetry

$$N_N = \eta L N, \quad N_D = \eta L D$$
: event counts

$$\delta A^{\text{exp}} = \frac{\delta P_{e^-}}{P_{e^-}} A^{\text{exp}} \oplus \frac{\delta P_{e^+}}{P_{e^+}} A^{\text{exp}} \oplus \frac{1}{P_{e^-} - P_{e^+}} \frac{1}{\sqrt{N_D}}$$

$$\mathcal{S} = \frac{A^{\text{exp}}}{\delta A^{\text{exp}}}$$

$P_{e^-} = 80\%$ ,  $P_{e^+} = 30\%$ , 3% relative uncertainties,

$L = 10 \text{ ab}^{-1}$ ,  $\eta = 80\%$  (100%) for  $b\bar{b}$  ( $WW$ )

# Probing $y_e$ via transverse spin asymmetries at the FCC-ee

Realistic experimental cuts:

$$5^\circ < \theta < 175^\circ \text{ for } b\bar{b}$$

$$E_{j_1,j_2} < 52, 45 \text{ GeV}, E_\ell > 10 \text{ GeV}, E_{\text{miss}} > 20 \text{ GeV}, m_{\ell\nu} > 12 \text{ GeV} \text{ for } WW$$

Optimization cuts:

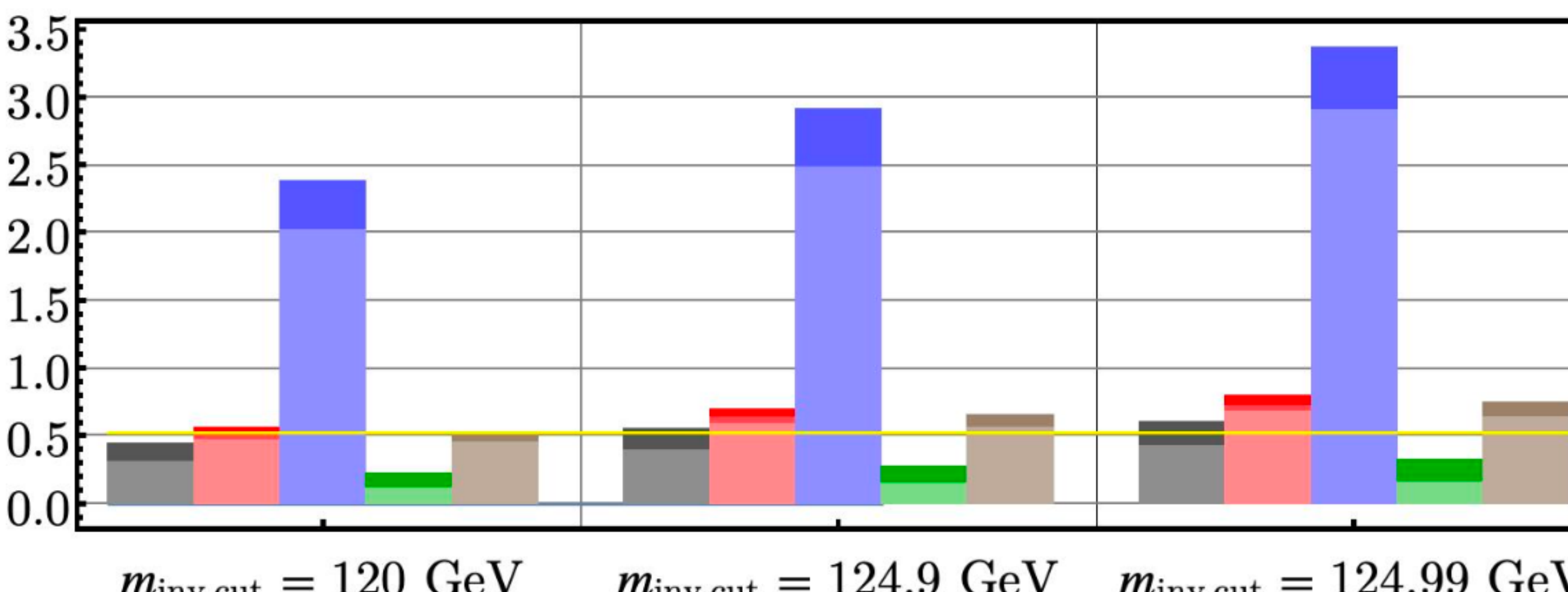
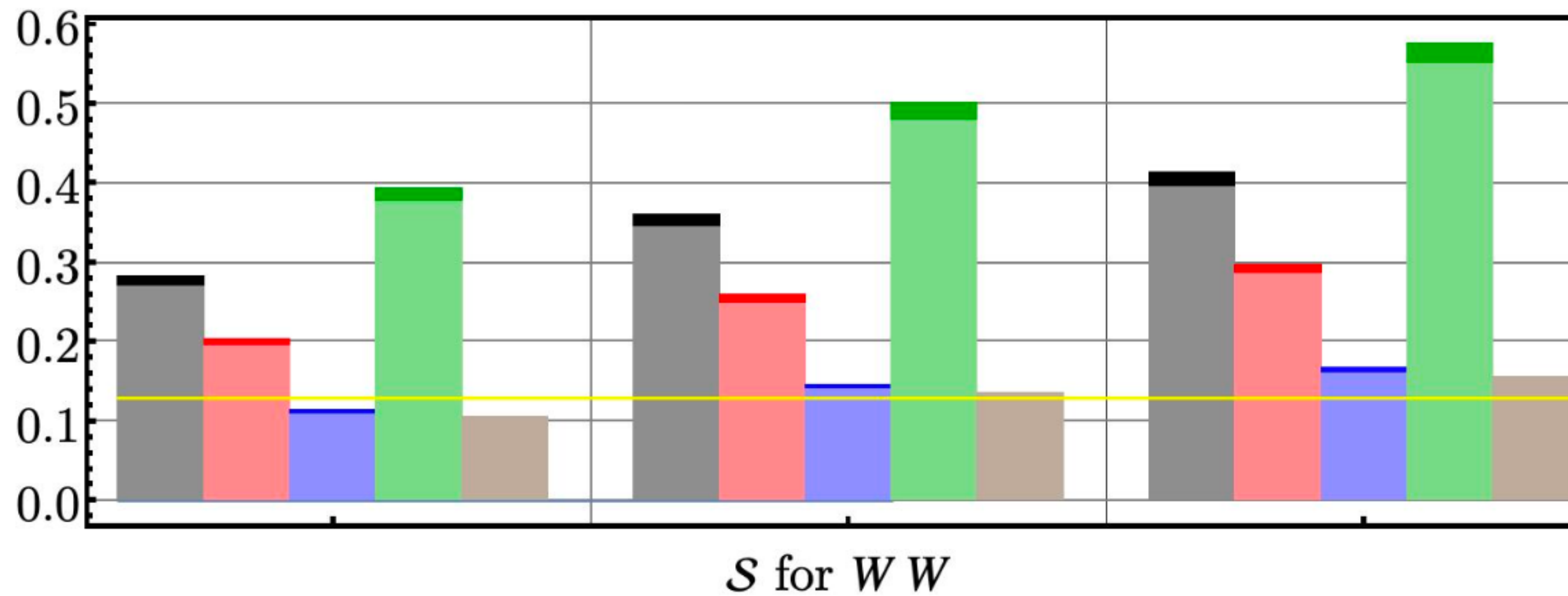
$$m_{\text{inv}} > m_h - x\Gamma_h$$

$$39\% \text{ symmetric cut on } \theta \in [0, 180^\circ] \text{ for } b$$

$$28\% \text{ symmetric cut on } \theta \in [0, 180^\circ] \text{ for } W(\ell\nu)$$

# Probing $y_e$ via transverse spin asymmetries at the FCC-ee

$\mathcal{S}$  for  $b\bar{b}$



■ DP ■  $\text{SP}^0$  ■  $\text{SP}^+$  ■  $\text{SP}^-$  ■ Reference

dark: optimization cuts  
light: no optimization cuts

$$\text{Reference} = \frac{\text{signal}}{\sqrt{\text{background}}}$$

using inclusive xsection

Yellow line: from inclusive xsection using boosted decision tree analysis to remove background, from d'Enterria+ [2107.02686]

A scenic landscape featuring a winding river flowing through rolling green hills. In the foreground, a white paved path runs parallel to a set of train tracks. On the left, there's a cluster of buildings and utility poles. The background is filled with dense green trees and foliage under a clear blue sky.

Coda

# Summary

- Motivation: Can future colliders, via precision observables, reveal or constrain BSM physics?
- Collider diversity = different tools needed for different bolts: Each collider targets a different direction in SMEFT parameter space. Together, they close gaps no single machine can.
- DIS (EIC, LHeC, and FCC-eh): Covers distinct kinematic regimes. When combined, they lift flat directions in global fits and set powerful bounds on new interactions.
- DY (HL-LHC): Pushes high invariant mass tails ( $m_{\ell\ell} \gg m_Z$ ) with enormous statistics, testing SMEFT directions beyond the reach of LEP or low-energy DIS.
- $e^+e^-$  (FCC-ee): Precision machine par excellence. Clean initial state. Sensitive to subtle couplings like the electron Yukawa.

# Summary

What's the point of constraining SMEFT parameters?

- *We haven't found new particles yet:* New physics must be either too heavy to produce or too weakly coupled to resolve.
- *But new physics still leaves footprints:* Even if we can't see the particles, we can detect their effect as tiny deviations in precision observables.
- *SMEFT is our translator:* It tells us how unknown heavy physics would subtly deform SM predictions:
  - Deviations are encoded in Wilson coefficients.
  - Constraining these coefficients = testing every possible UV completion, all at once.

# Contributions

Papers:

- R. Boughezal, A. Emmert, T. Kutz, S. Mantry, M. Nycz, F. Petriello, K. Şimşek, D. Wiegand, X. Zheng, *Neutral-current electroweak physics and SMEFT studies at the EIC*, Phys. Rev. D **106** (2022) 016006, arXiv:2204.07557
- C. Bissolotti, R. Boughezal, K. Şimşek, *SMEFT probes in future precision DIS experiments*, Phys. Rev. D **108** (2023) 075007, arXiv:2306.05564
- R. Boughezal, F. Petriello, K. Şimşek, *Transverse spin asymmetries and the electron Yukawa coupling at an FCC-ee*, Phys. Rev. D **110** (2024) 075026, arXiv:2407.12975
- DY+jet project: in progress

Other publications:

- R. Abdul Khalek *et al.*, *Snowmass 2021 White Paper: Electron Ion Collider for high energy physics*, arXiv:2203.13199
- C. Bissolotti, R. Boughezal, K. Şimşek, *SMEFT analysis with LHeC, FCC-eh, and EIC DIS pseudodata*, DIS2023 Proceedings, arXiv:2307.09459

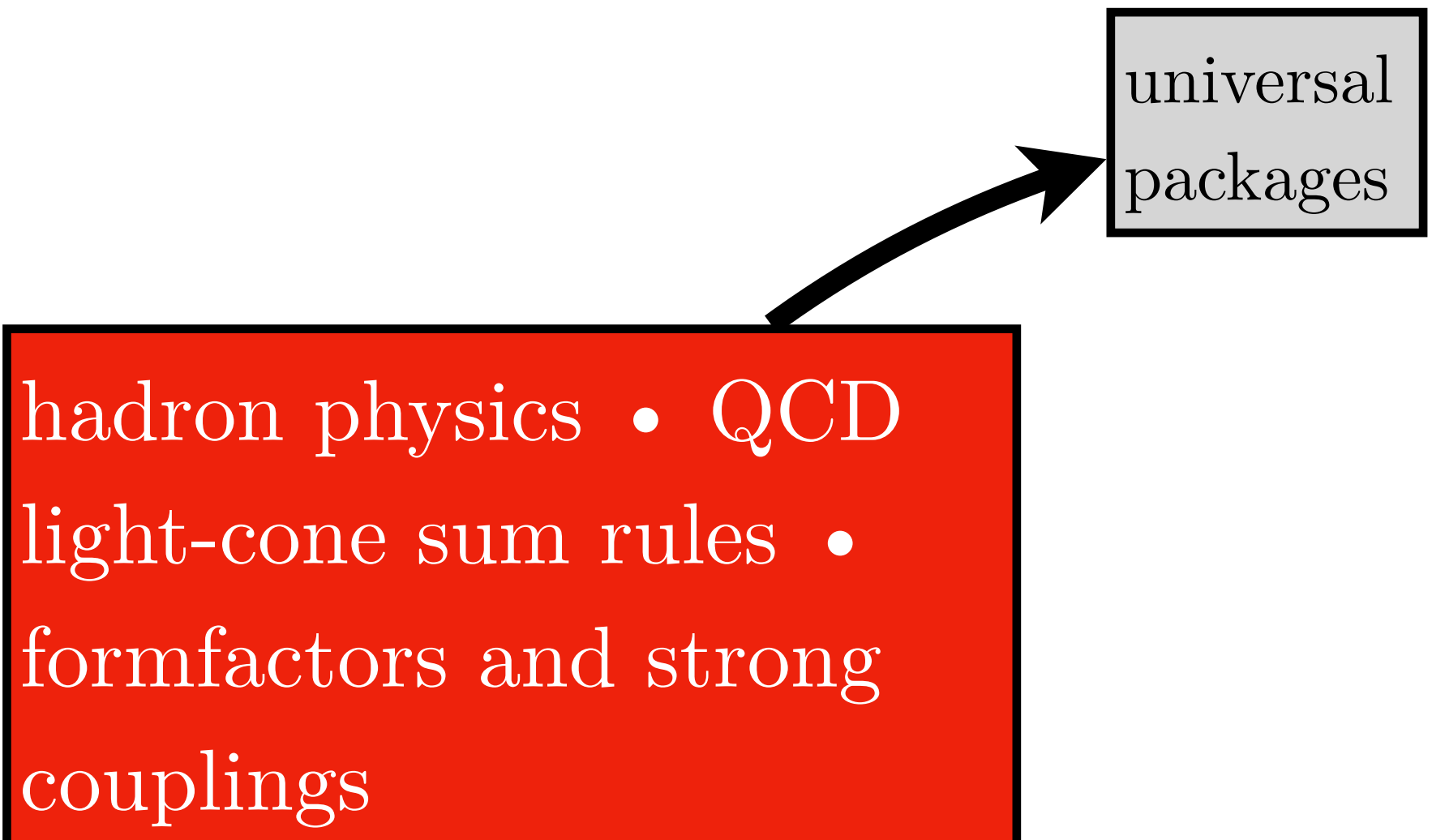
# Outlook and future directions

# Outlook and future directions

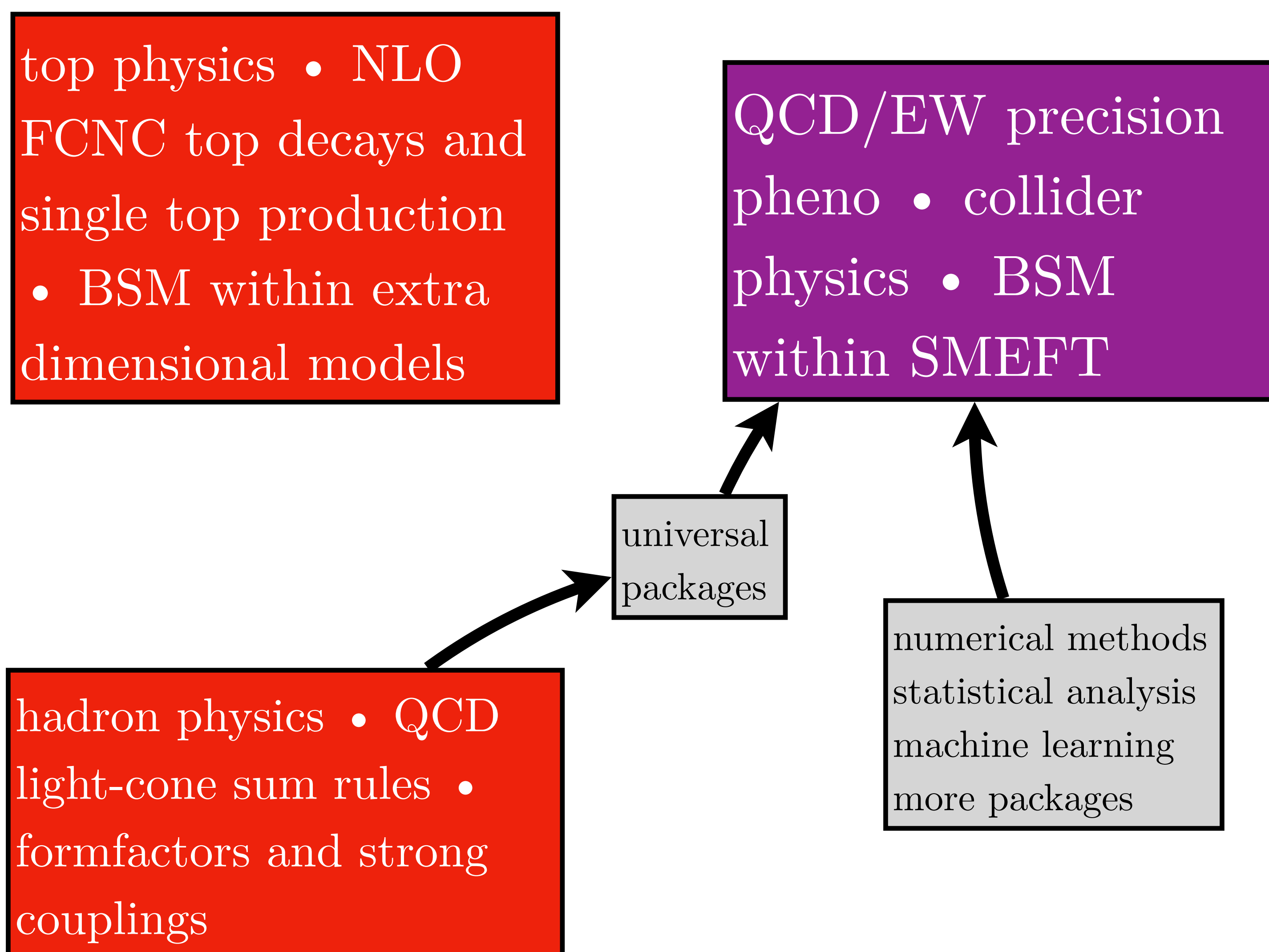
top physics • NLO  
FCNC top decays and  
single top production  
• BSM within extra  
dimensional models

# Outlook and future directions

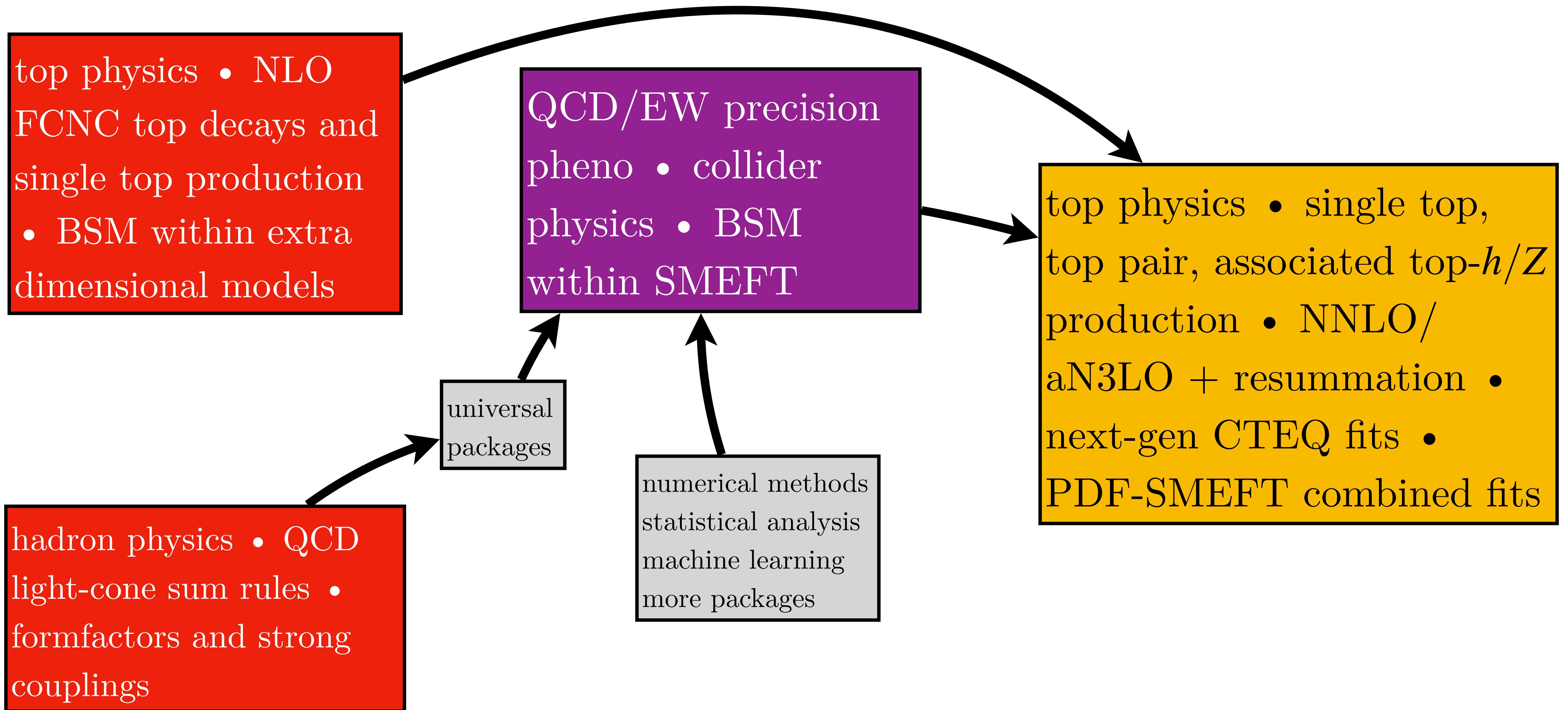
top physics • NLO  
FCNC top decays and  
single top production  
• BSM within extra  
dimensional models



# Outlook and future directions



# Outlook and future directions



Thank you.